Hindawi
Wireless Communications and Mobile Computing
Volume 2021, Article ID 8844630, 20 pages
https://doi.org/10.1155/2021/8844630

Research Article

A Novel Deceptive Jamming Approach for Hiding Actual Target and Generating False Targets

Shahid Mehmood,[1] Aqdas Naveed Malik,[1] Ijaz Manssor Qureshi,[2] Muhammad Zafar Ullah Khan,[1] and Fawad Zaman [3]

[1]*Department of Electrical Engineering, International Islamic University, Islamabad, Pakistan*
[2]*Department of Electrical Engineering, Air University Islamabad, Pakistan*
[3]*Department of Electrical & Computer Engineering, COMSATS University Islamabad, Pakistan*

Correspondence should be addressed to Fawad Zaman; fawad.zaman@comsats.edu.pk

Received 6 August 2020; Revised 2 March 2021; Accepted 24 March 2021; Published 7 April 2021

Academic Editor: Cong Pu

Deceptive jamming is a popular electronic countermeasure (ECM) technique that generates false targets to confuse opponent surveillance radars. This work presents a novel approach for hiding the actual target while producing multiple false targets at the same time against frequency diverse array (FDA) radar. For this purpose, the modified FDA radar is assumed to be mounted on the actual aircraft. It intercepts the opponent's radar signals and transmits back to place nulls in the radiation pattern at the desired range and direction to exploit FDA radar's range-dependent pattern nulling capability. The proposed deceptive jammer produces delayed versions of the intercepted signals to create false targets with multiple ranges to confuse the opponent's radar system. The novel mathematical model is proposed whose effectiveness is verified through several simulation results for different numbers of ranges, directions, and antenna elements.

1. Introduction

Modern warfare is information and electronic based, which is evidently replacing the conventional platforms [1]. It requires no further confrontation between soldier to soldier, trench to trench, platoon to platoon, and platform to platform; rather, it relies on nonlinear and nonsymmetric war between system to system [2]. As the 21st century unfolds, the concept of electronic information warfare has become center of the gravity in which the radar system constitutes the key components that provide early warning capabilities [3]. Radar works as an early warning system and bestows extra time space to react against imminent threat. The principle of the radar to detect the desired target is transmitting radio waves towards the target and calculates round-trip time of the reflected waves after striking with the target [3]. To counter enemy radars, ECM techniques (also known as radar jamming techniques) were introduced [4]. These techniques are used to deny the important information about the desired aircrafts (direction of arrival, range, velocity, etc.) that any foe radar seeks [4]. In the presence of strong electronic counter measure (radar jammers) systems, it is difficult to detect the target aircraft; but there are many electronic counter-countermeasure (ECCM) techniques available in literature to counter radar jammer and to locate correctly the target [5, 6]. Some ECCM (which are also known as antijamming) systems steer nulls towards strong interfering signals to secure own functioning.

Mainly, there are two types of radar jamming techniques: mechanical methods (passive jamming) and electrical methods (active jamming) [3]. In mechanical methods, physical means like chaffs, decoys, corner reflectors, and stealth are used in securing the desired aircrafts' flights and to deceive enemy radars [4]. These physical means of radar jamming are traditional techniques which are not so effective. Electrical methods of radar jamming are effective and still in use [1, 2]. These methods can be categorized in two types: barrage jamming (also known as noise jamming) and deceptive jamming

[4]. Barrage jamming methods use radar jammers to put huge powers across the desired spectrum of the frequencies which blankets the radar's display to interrupt its normal functioning [7]. There are two main reasons of the ineffectiveness of this type which is huge power losses for longer periods of times, and even it cannot cover the entire frequency spectrum at the same time [8]. The deceptive jamming mode is used to deceive the enemy radars by showing them multiple very similar fake targets with different aircraft attitudes (range, direction, velocity, acceleration, etc.) [9].

This paper focuses only on the deception jamming, because this is the most effective way to secure the flight of the desired aircraft from the enemy radars by showing congruent false targets [10]. Therefore, implementing effective and efficient deceptive jamming (DJ) techniques has become a hotspot area of research in radar electronic countermeasures [11, 12]. Many methods have been developed in the modern literature [13–15]. In pursuit of deceptive radar jamming, the simplest way to generate multiple false targets is to hold enemy radar signals and after doing time-modulation transmit those signals back to the enemy radar [16]. When the enemy radar receives these signals, it will perceive multiple false targets with different ranges, but with the same direction along with the actual target. A modest contribution has been made using target pose and motion information to generate false targets in [17]. To deceive the opponent radar with a number of fake targets, another effort has been made in [18] using micromotion characteristics, but both have the same issue of computation complexity.

Multiple false targets also have been achieved using electromagnetic properties (EM model modulation) and translation modulation in [19]. By exploiting the concept of sub-Nyquist sampling theorem, a series of multiple fake targets have proposed in [20, 21]. Another remarkable approach has been defended to produce multiple false targets using product modulation in which an offline deceptive signal template is produced and then multiplied with enemy radar signal in [22]. Interrupted-sampling repeater jamming (ISRJ) establishes a novel approach to generate deception jamming by allowing the single radar antenna jammer to sample periodically and iterating a fraction of the intercepted enemy radar signal [23]. Inappropriately, high complexity and large computation is the main drawback of inefficiency of the above deceptive techniques in the field of electronic countermeasures. Further, these techniques are also unable to hide real target.

A recent effort has been exercised to achieve the goal by adding escort-free flight jammer drone ahead of the actual aircraft based on periodic the 0-π phase modulation which neutralizes the effectiveness of the enemy radar by displaying its multiple verisimilar false targets [24]. The escort-free flight jammer intercepts enemy radar signals and after doing phase modulation in the periodic 0-π sequence, these signals are retransmitted towards the actual target, whereby these are scattered towards the enemy radar and present multiple false targets with different ranges [24], but it considers the scenario where a separate escorting drone jammer is required which is not feasible in most practical situations.

Against to the only angle-dependent beam scanning techniques, FDA is an efficient beam scanning array used for phased array radars which has recently got tremendous attention in literature due to its greater achievement of wide angle coverage [25–28]. The radiation pattern of the phase array radar (PAR) depends only upon the direction while FDA radiation pattern depends upon the direction and range, due to its diversity in frequency across the array elements. Hence, FDA radiation pattern is capable of null steering to the particular range and direction. FDA is implemented by applying small increment in frequencies across array elements to achieve range angle-dependent beam scanning transmission [29, 30]. Hence, it enables beam scanning without need of any phase shifters and physical steering [31–33].

A good effort in field of deceptive jamming is explored in [34] which utilizes frequency diverse array. It produces multiple fake targets at different distances across the slant range but at the same azimuthal range aligned with the actual target. The technique is unable to draw false targets at different azimuthal ranges other than azimuthal range of the actual target. A novel approach in the field of deceptive jamming has been introduced in [35] with wave scattering using FDA for space-borne synthetic aperture radar (SAR). This approach considers the scenario where we offer deceptive jamming to the opponent radar for securing our valuable targets in its own territory with the help of placing deceptive reflectors. But this technique provides no solution to tackle the opponent radar operating from its own territory without the help of any ground-based situated wave scattering reflectors. Further, this method is also unable to hide its own target from the enemy foresight.

Although a modest effort has been made in [36] to introduce the deceptive jamming approach through frequency diversity, there are a few shortcomings in the proposed technique. These include (a) that deceptive jammer should be synchronized/attached or working in collaboration with a friendly GPS satellite system, (b) deceptive jammer must have prior knowledge of the location in space of the opponent radar, (c) the method is slow because it is using FFT and IFFT to convert signals from time domain to frequency domain and then back to previous domain, which makes it performance slow, and (d) it does not give any solution if the foe radar is also an FDA radar.

Paper in the reference [37] presented a deception jamming method which generates multiple scenes (multiple false targets) using FDA radar antenna, where number of false targets depend on the number of antenna array elements. The technique in reference [38] uses the simplest way to generate nulls towards the desired direction and range in order to suppress the offered range-angle dependent interference jamming, but this technique is unable to offer deceptive jamming to confuse the opponent radar, and it also does not hide its own target from the vision of the opponent radar. Further, as we know that FDA is time, angle, and range-dependent, but in this technique, the time-dependency factor of the FDA radar is diminished by considering it as zero ($t = 0$), which is not an appropriate for the practical scenarios [38].

Until now, best to the authors' knowledge, available deceptive jamming techniques in the present literature are not dealing with the hiding of the actual target along the generation of false targets using FDA radars. Present literature

also does not offer deceptive jamming for the opponent radars which work on FDA radar principle. The proposed study would investigate these limitations in depth and subsequently would present a probable solution against it. The main contribution of the work is summarized below.

(i) This research produces a novel deceptive jamming approach in the field of ECM

(ii) The algorithm works against the opponent FDA radar and hides the actual target from it

(iii) For this purpose, enemy radar pulse is captured by the target FDA radar, and null is placed at the radar range to hide its own target alongside after its time modulation

(iv) It is equally effective to tackle ground-based opponent FDA radar in its own territory

(v) The proposed technique efficiently works without help of ground-based wave-scattering reflectors or advance escort-free-drone jammers

(vi) The proposed algorithm also confuses the opponent FDA radar by multiple false targets at different user-defined ranges

The remaining part of the paper is organized in the following way. Sections 2 and 3 introduce mathematical background of the FDA radar and comparison with existing techniques, respectively. Section 4 depicts the proposed method to secure the flight of the actual aircraft in the enemy territory by neutralizing the dangers of enemy radars, while Section 5 shows the effectiveness and correctness of the proposed techniques via simulations in three dimensions and in two dimensions for four different cases. Finally, conclusion of the paper has been presented in Section 6.

2. Data Model for the FDA Radar

FDA radar uses small increment in frequency of each element over the antenna array. Radiation pattern of the FDA radar is a function of range, angle, and time [25–28]. FDA radar implements waveform diversity among the radiating elements which brings more functionality [29, 30]. Figure 1 depicts an FDA that consists of uniform linear array (ULA) having n-isotropic radiating elements. The distance d between any two adjacent elements is taken same with the uniform current distribution. The carrier frequency of each element is incremented by a small constant frequency offset [31]. The simplest monochromatic signal is assumed to be transmitted from the nth element of the array, and it can be mathematically expressed as [32]

$$s_n(t) = \exp\ (j2\pi f_n t), \tag{1}$$

where f_n is the frequency of the nth element as $f_n = f_0 + (n-1)\Delta f$ for $n = 1, \cdots, N$. Similarly, f_0, Δf, and N represent carrier frequency, a small constant frequency increment, and total number of elements, respectively, in the FDA array. When signal of the nth element reaches at a far-field location after time t_0 with range R_1 (reference to the first element in the array) and azimuth direction θ, its radiating beam can be represented as [31]

$$s_n(t - t_0) = \exp\ \{j2\pi f_n(t - t_0)\}. \tag{2}$$

For $t_0 = R_n/c$, (2) can be expressed as

$$s_n\left(t - \frac{R_n}{c}\right) = \exp\ \left\{j2\pi f_n\left(t - \frac{R_n}{c}\right)\right\}, \tag{3}$$

where c stands for the speed of light and $R_n = R_1 - (n-1)dsin(\theta)$ shows the distance from the nth element of the array to the target location. The array factor (AF) for FDA can be written as [32]

$$AF = \sum_{n=0}^{N-1} \exp\left\{j2\pi f_n\left(t - \frac{R_n}{c}\right)\right\}. \tag{4}$$

After placing values of f_n and R_n, (4) becomes as

$$AF = \exp\ \{j\psi_0\} \sum_{n=0}^{N-1} \exp\left\{j\frac{2\pi n}{c}\Phi\right\}, \tag{5}$$

where $\Phi = c\Delta f t - \Delta f R + df_0 sin\theta + n\Delta f d sin\theta$.

$$AF \cong \exp\ \{j\psi_1\} \frac{\sin\ [(N\pi/c)\Phi]}{\sin\ [(\pi/c)\Phi]}, \tag{6}$$

where ψ_0 stands for $2\pi f_0\ (t - R_1/c)$ and ψ_1 stands for $\psi_0 + \pi(N-1)[\Delta f R_1/c - (df_0\ sin\theta)/c - \Delta f d sin\theta/c]$, while n^2 of the fourth term $(n^2(\Delta f d \sin\theta/c))$ has been replaced by n in the fourth term $(n(\Delta f d \sin\theta/c))$ of the last expression of the AF to achieve closed form expression. So, the problem in hand is how to hide actual aircraft target from the effectiveness of the opponent FDA radar along with generation of multiple fake deceptive targets at different ranges in the direction of actual aircraft using the ULA-based FDA radar.

3. Comparison with Existing Techniques

The three deceptive jamming techniques [34–36] are selected for comparison. All of these techniques use frequency diverse arrays to generate multiple false targets. A deceptive jamming technique which is explored in [34] utilizes frequency diverse array. It generates multiple false targets at various distances across the slant range but at the same azimuthal range which aligned with the actual target as shown in the simulation (Figure 2). A good effort [35] has been made in the field of deception jamming using FDA which generates multiple fake targets at different positions in the slant range and azimuthal range to confuse the opponent radar.

Four elements array with adjacent distance of half wavelength were used in FDA with frequency offset 500 kHz, and its simulation of [35] is shown in Figure 3, which reflects actual target at slant range 7500 m and azimuthal range 0 m along with four false targets which are situated at slant ranges

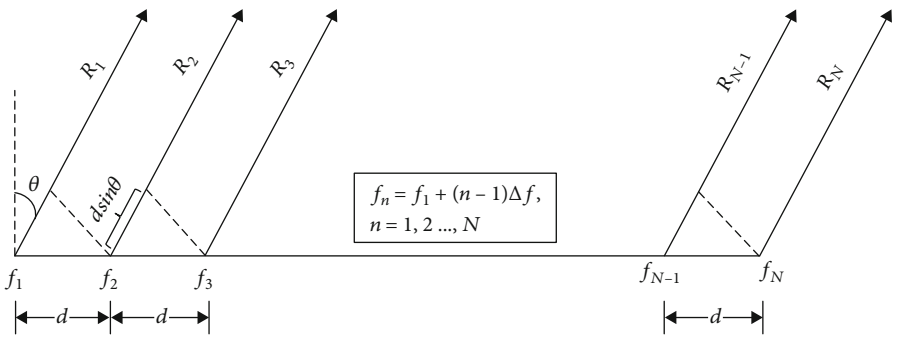

Figure 1: Geometry of the FDA radar uniformly linearly polarized with n elements.

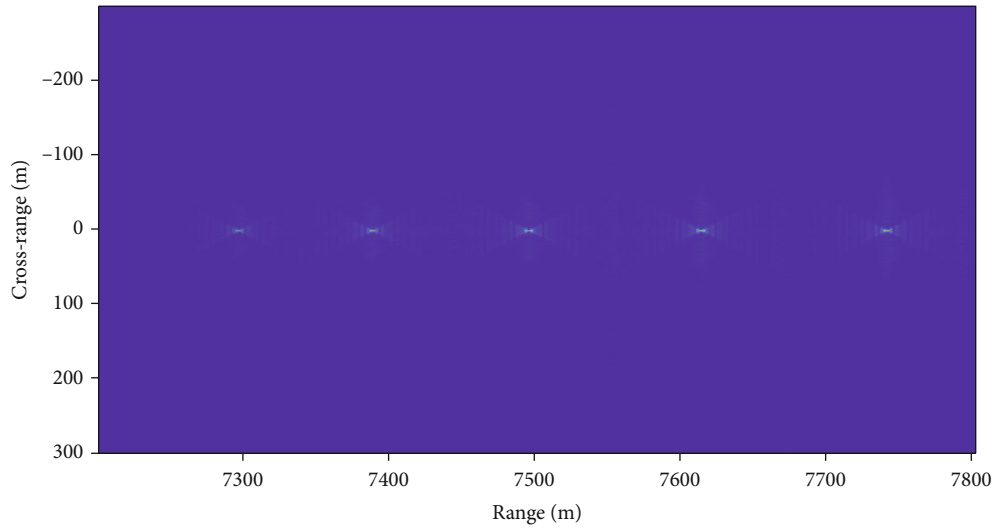

Figure 2: Actual target at (7500, 0) and false targets at {(7300, 0), (7395, 0), (7615, 0), and (7750, 0)} [34].

7300 m, 7395 m, 7615 m, and 7750 m with azimuthal range at 100 m. Figure 4 shows the effectiveness of the technique [36] by considering the jammer at the middle of the scene (7500 m, 0 m); this algorithm generates four false targets at different locations. Algorithm assumes FDA array of eight elements with frequency offset 300 kHz. It is evident from Figures 2–4 that although all three techniques [34–36] are big achievement in the field of deception jamming using frequency diverse array, none is able to hide actual target alongside generating multiple false targets.

4. Proposed Method

The key idea behind this research is to interrupt enemy radar signals and then using these signals (after proposed modifications), we hide our object (aircraft) along with generating multiple fake targets. We assumed that the proposed (modified FDA) radar is mounted on the target aircraft, and the opponent radar is placed on the ground as shown in scenario Figure 5. In purpose of hiding its own target aircraft, the interrupted signal of the opponent radar will be transmitted back after desired changes to place null at the range and the direction of the foe radar receiver. In the current scenario, it is assumed that the opponent radar is capable of transmitting and receiving FDA radiation patterns. In order to deceive the enemy radar with multiple fake targets, time-delayed replicas of the received signal will be sent towards the enemy radar. The graphical abstract of the proposed method is shown in Figure 6

4.1. Actual Target Hiding. In this section, the mathematical model is formulated to hide the actual target. Let the radiated signal from the *nth* element of the enemy FDA radar which is given as

$$s_n(t) = \exp\{j2\pi f_n t\},\ 0 \le t \le T, \tag{7}$$

where t is the time indexing within the radar pulse width T. We assume that the enemy radar is situated at distance r and at direction θ from the target. The enemy radar transmitted signal from *nth* element is received at *mth* element of the target FDA radar that can be expressed as

$$y_{m,n}(t - \tau_{m,n}) = \exp\left\{j2\pi f_n(t - \tau_{m,n})\right\}, \quad m = 1, 2 \cdots N, \tag{8}$$

where $\tau_{m,n} = [r - (n-1)d \sin\theta + d(m-1) \sin\theta]\, 1/c$. Generally, (8) can be given as

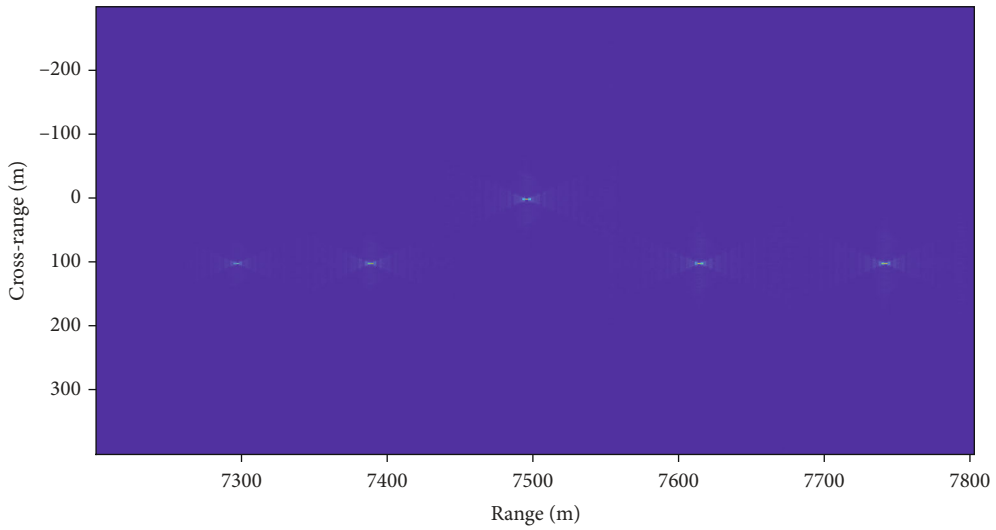

Figure 3: Actual target at (7500, 0) and false targets at {(7300, 100),(7395, 100),(7615, 100),and (7750, 100)} [35].

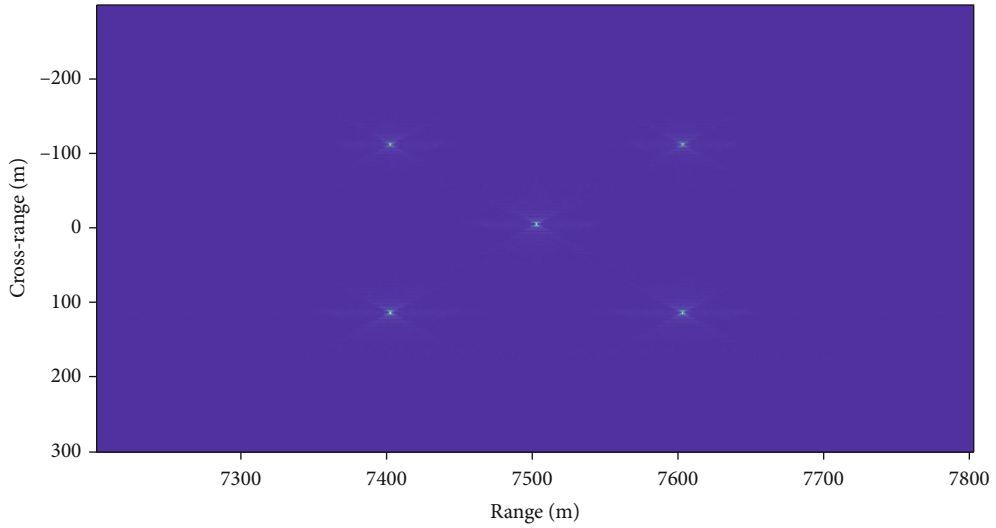

Figure 4: Actual target at (7500, 0) and false targets at {(7400, -100),(7400, 100),(7600, -100),and (7600, 100)} [36].

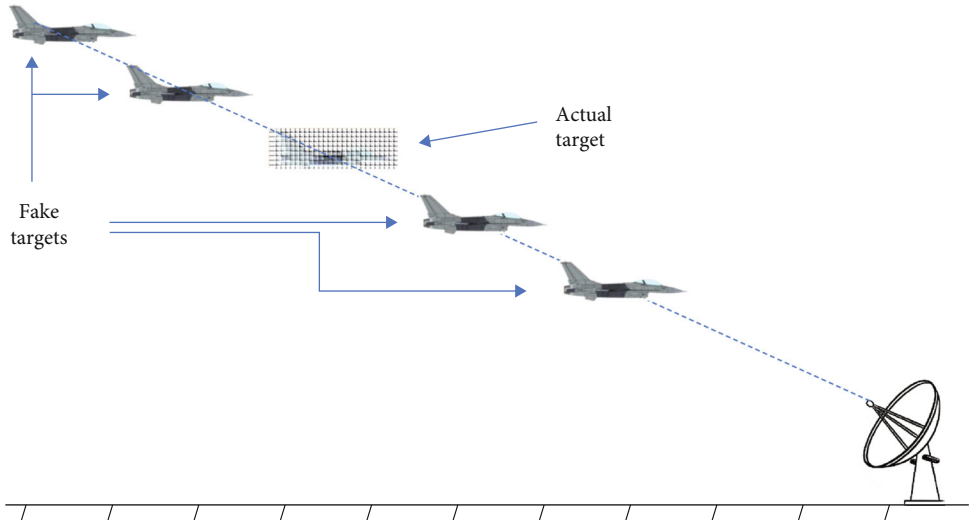

Figure 5: Proposed and adopted scenario.

$$y_m = \sum_{n=1}^{N} \exp\{j2\pi f_n(t-\tau_{m,n})\}. \quad (9)$$

Hence the received signal can be decomposed after processing through matched filtering with $\exp^*\{j2\pi f_n t\}$ as processed below.

$$\begin{aligned} y'_{m,n} &= \exp\{j2\pi f_n(t-\tau_{m,n})\} \times \exp^*\{j2\pi f_n t\}, \\ &= \exp\{j2\pi f_n t - j2\pi f_n \tau_{m,n} - j2\pi f_n t\}, \\ &= \exp\{-j2\pi f_n \tau_{m,n}\}. \end{aligned} \quad (10)$$

After placing values of $\tau_{m,n}$ and f_n, the expression becomes

$$y'_{m,n} = \exp\left\{-j2\pi (f_0 + (n-1)\Delta f)\left([r-(n-1)d\sin\theta + d(m-1)\sin\theta]\frac{1}{c}\right)\right\}, \quad (11)$$

$$= \exp\left\{-j2\pi\left[\frac{f_0 r}{c} - \frac{f_0(n-1)d\sin\theta}{c} + \frac{f_0(m-1)d\sin\theta}{c} + \frac{(n-1)\Delta f r}{c} - \frac{(n-1)^2\Delta f d\sin\theta}{c} + \frac{(n-1)(m-1)\Delta f d\sin\theta}{c}\right]\right\}. \quad (12)$$

Last two terms are insignificant; so these, terms are ignored.

$$\begin{aligned} y''_{m,n} &= \exp\left\{-j2\pi\frac{f_0 r}{c}\right\} \times \exp\left\{j2\pi\frac{f_0(n-1)d\sin\theta}{c}\right\} \\ &\quad \times \exp\left\{-j2\pi\frac{f_0(m-1)d\sin\theta}{c}\right\} \\ &\quad \times \exp\left\{-j2\pi\frac{(n-1)\Delta f r}{c}\right\}, \\ &= \exp\left\{-j2\pi\frac{r}{\lambda_0}\right\} \times \exp\left\{j2\pi\frac{(n-1)d\sin\theta}{\lambda_0}\right\} \\ &\quad \times \exp\left\{-j2\pi\frac{(m-1)d\sin\theta}{\lambda_0}\right\} \\ &\quad \times \exp\left\{-j2\pi\frac{(n-1)\Delta f r}{c}\right\}, \\ &= \exp\left\{-j2\pi\frac{r}{\lambda_0}\right\} \sum_{n=1}^{N} \exp\left\{-j2\pi\frac{\Delta f}{c}(n-1)r\right\} \exp \\ &\quad \cdot\left\{j2\pi\frac{d}{\lambda_0}(n-1)\sin\theta\right\} \\ &\quad \exp\left\{-j2\pi\frac{d}{\lambda_0}(m-1)\sin\theta\right\}. \end{aligned} \quad (13)$$

For simplicity, outside factor is eliminated.

$$y'_{m,n} = \exp\left\{-j2\pi\frac{\Delta f}{c}(n-1)r\right\} \exp\left\{j2\pi\frac{d}{\lambda_0}(n-1)\sin\theta\right\} \exp \cdot\left\{-j2\pi\frac{d}{\lambda_0}(m-1)\sin\theta\right\}. \quad (14)$$

Alternatively,

$$y'_m = \sum_{n=1}^{N} \exp\left\{-j2\pi\frac{\Delta f}{c}(n-1)r\right\} \exp\left\{j2\pi\frac{d}{\lambda_0}(n-1)\sin\theta\right\} \exp \cdot\left\{-j2\pi\frac{d}{\lambda_0}(m-1)\sin\theta\right\}, \quad (15)$$

where the first factor of the above expression dictates phase shift caused by the target range, and rest factors reflect phase shifts caused by the direction and different wave paths due to physical displacement diversity of the target and the source array elements. Now, the expression $y'_{m,n}$ can be recomposed into these factors in this form.

$$y_{m,n} = \mathrm{a_n}(\mathrm{r})\mathrm{a_n}(\theta)\mathrm{b_m}(\theta), \quad (16)$$

where $a_n(r) = \exp\{-j2\pi(\Delta f/c)(n-1)r\}$,

$$a_n(\theta) = \exp\left\{j2\pi\frac{d}{\lambda_0}(n-1)\sin\theta\right\},$$

$$b_m(\theta) = \exp\left\{-j2\pi\frac{d}{\lambda_0}(m-1)\sin\theta\right\}. \quad (17)$$

Now, we can transform the above received snapshot expression into vector form as

$$\begin{aligned} \mathbf{Y}_s &= [y_{11}, y_{12}, \cdots, y_{1N}, y_{21}, y_{22}, \cdots, y_{2N}, \cdots\cdots\cdots, y_{N1}, y_{N2}\cdots, y_{NN}]^T, \\ &= \mathbf{b}(\theta)\otimes\mathbf{a}(r,\theta), \end{aligned} \quad (18)$$

where $\mathbf{Y}_s \in \mathbb{C}^{N^2\times 1}$, $\mathbf{b}(\theta) \in \mathbb{C}^{N\times 1}$, and $\mathbf{a}(r,\theta) \in \mathbb{C}^{N\times 1}$. The superscript T and $\otimes$ reflect transpose and Kronecker product operators, respectively. The vector $\mathbf{a}(r,\theta)$ can be decomposed further in this way

$$\mathbf{a}(r,\theta) = \mathbf{a_r}(r)\odot\mathbf{a_\theta}(\theta), \quad (19)$$

where $\mathbf{a_r}(r) \in \mathbb{C}^{N\times 1}$ and $\mathbf{a_\theta}(\theta) \in \mathbb{C}^{N\times 1}$ are the range and angular steering vectors, respectively. The $\odot$ is called Hadamard product operator which reflects element-wise product between vectors. After applying DOA (direction of arrival) and range algorithms, one can find direction and range of the enemy radar, but this is beyond the scope of our research.

Now, in order to hide our target from the enemy radar, we have to transmit back the processed received signal towards the enemy radar carrying the desired information of range and direction of the enemy radar, but without considering the 3rd factor, which is not part of the deceptive jamming transmission propagation. Hence, the desired signal structure will become as follows:

$$y_n = \exp\left\{-j2\pi\frac{\Delta f}{c}(n-1)R_0\right\} \exp\left\{j2\pi\frac{d}{\lambda_0}(n-1)\sin\theta_0\right\}, \quad (20)$$

where $\theta_0 \& R_0$ are direction and range of the enemy radar, respectively. We can simplify it further in this way.

$$\boldsymbol{Y}_t = \sum_{n=1}^{N} \exp\left\{ j(n-1)\left[\frac{2\pi}{c}(\mathrm{f}_0 \mathrm{dsin}\theta_0 - \Delta f R_0)\right]\right\}. \quad (21)$$

Now, first we will verify the above result using simpler way, and then we will place null in the desired radiation pattern at a certain direction and range to cover our target. The generalized phase difference between any two elements of the FDA radar is found as

$$\Delta\varphi_{n-1,n} = \frac{2\pi d \sin\theta}{\lambda_0} - \frac{2\pi\Delta f R_1}{c} + \frac{(2n-3)2\pi\Delta f d \sin\theta}{c}. \quad (22)$$

In (22) the 3rd term which is insignificant, it can be ignored.

$$\Delta\varphi_{n-1,n}(R_1,\theta) = \frac{2\pi d \sin\theta}{\lambda_0} - \frac{2\pi\Delta f R_1}{c} = \frac{2\pi}{c}(f_0 d \sin\theta - \Delta f R_1). \quad (23)$$

The AF at range R_1 and direction θ from the radar can be expressed as

$$AF = \sum_{n=1}^{N} \exp\left\{ \mathrm{j(n-1)}\left[\frac{2\pi}{\mathrm{c}}(\mathrm{f}_0 \mathrm{dsin}\theta - \Delta f R_1)\right]\right\}. \quad (24)$$

It is considered that the enemy radar is situated at range R_0 and angle θ_0 from the target. Then, we assume that the interrupted waveform with carrier frequency f_0 can be expressed as below.

$$\mathrm{AF}(R_0,\theta_0) = \sum_{n=1}^{N} \exp\left\{ \mathrm{j(n-1)}\left[\frac{2\pi}{\mathrm{c}}(\mathrm{f}_0 \mathrm{dsin}\theta_0 - \Delta f R_0)\right]\right\}. \quad (25)$$

Now, this is the desired expression, and it is the same equation that we have concluded before. Hence, the expression of the derived AF is same to the signal which is meant for transmission towards the enemy radar. Using this AF, a null will be placed at desired range and direction to hide its own target from the vision of the enemy radar. At the end of this section, the above AF will be factorized in order to find weights for placing null at $R_0 \& \theta_0$. Now, we will explain how to generate null at R_0 by considering the simplest case. From the above expression, it is evident that the interelement phase difference is the same for the whole array between all adjacent elements; so, we can rewrite the above expression of the phase difference in the following way. After getting knowledge of above expressions, AF of the diverse frequency array can be modeled in the following way.

$$\mathrm{AF} = \sum_{n=1}^{N} z^{n-1}, \quad (26)$$

where $z = \exp(j\psi)$, $\psi = \alpha + \beta + \gamma$, $\alpha = 2\pi f_0 d \sin\theta_0/c$, and $\gamma = -2\pi\Delta f R_0/c$. Extra term β was added into the AF to get scanning capabilities. In standard practices, usually, β is added in the desired AF to steer the radiation patter of the desired communication.

The above expression is the simplest form of the AF for the FDA antenna arrays, which has fix the main beam direction and null directions. Steering of the beam pattern for such an array is not possible. In other words, to get control over the nulls of the radiation pattern, we need to plug in and update weights of the expression. Now, to steer the beam pattern (main beam and nulls) of the frequency diverse array, appropriate weights are necessary. Further, above AF must be put to equal to zero for the calculation of the appropriate weights to steer the beam pattern towards the desired directions.

$$AF = \sum_{n=1}^{N} A_{n-1} z^{n-1} = 0. \quad (27)$$

In determining of the weights, we considered the simplest case to avoid complexity of the proposed method. To find weights of the desired radiation pattern, we will follow this procedure.

$$AF = (z - r_0)\left(\sum_{n=1}^{N-1} z^{n-1}\right) = 0, \quad (28)$$

where $r_0 = e^{j(\alpha_0+\beta_s+\gamma_0)}$ is the desired null. Here, $\alpha_0 = (2\pi/c) f_1 d \sin\theta_0$, $\gamma_0 = -\Delta f R_0$, $\beta_s = (2\pi/c) f_1 d \sin\theta_s$, and θ_s are directions of the main beam. Then, the desired expression with updated weights will be as follows.

$$AF = \sum_{n=1}^{N} A_{n-1} z^{n-1}, \quad (29)$$

where $A_0 = -r_0$, $A_i = 1 - r_0$, $i = 1, 2, \cdots, N-2$, and $A_{N-1} = 1$. After applying these weights into the AF, we will be able to steer the null towards its desired direction θ_0 and range R_0. By following the above mechanism, our proposed method is capable of camouflaging its own target from the lethalness of the enemy radar.

4.2. Displaying Multiple Fake Targets. In second part of the proposed method, we will display multiple false targets to the enemy radar. For the purpose of multiple fake deceptive targets, we will process the received signal with two steps: first, the received signal will be time modulated with appropriate delays, and then power will be maximized and transmitted towards the enemy radar. We assume that the signal transmitted from the *nth* element of the enemy radar and received at the *mth* element of the false target generator (FTG) which is located at target that is

$$y_{j,m,n}(t) = \exp\left\{ j2\pi f_n \left(t - \tau_{j,m,n}\right)\right\}, \quad (30)$$

where

$$\begin{aligned}\tau_{j,m,n} &= \tau_j - \tau_{j,n} + \tau_{j,m},\\ &= \left[r_j - (n-1)d\sin\theta_j + (m-1)d\sin\theta_j\right]1/c\\ &= \left[r_j + (m-n)d\sin\theta_j\right]1/c.\end{aligned} \tag{31}$$

We suppose that the locally generated adjustable oscillator frequency is f_{FTG}; the receiving and processing time delay of the enemy radar signal is τ_{FTG}. Thus, the received signal can be down converted as follows.

$$y_{j,m,n} = \exp\left\{j2\pi f_n\left(t-\tau_{j,m,n}\right)\right\}\times\exp\left\{-j2\pi f_{\mathrm{FTG}}(t-\tau_{\mathrm{FTG}})\right\}. \tag{32}$$

As we know that our FTG is working on the principle of the frequency diverse array radar, so we can reflect that $f_{\mathrm{FTG}} = f_n$. After this change, the expression can be simplified in this way.

$$\begin{aligned}y_{j,m,n} &= \exp\left\{j2\pi f_n\left(t-\tau_{j,m,n}\right)\right\}\times\exp\left\{-j2\pi f_n(t-\tau_{\mathrm{FTG}})\right\},\\ &= \exp\left\{j2\pi f_n\left(\tau_{FTG}-\tau_{j,m,n}\right)\right\}.\end{aligned} \tag{33}$$

In order to generate multiple fake targets, signal will pass through the process of time modulation. Different time delays are made as follows.

$$\Delta\tau_{\mathrm{ft},i} = \frac{2\Delta r_{\mathrm{ft},i}}{c},\quad i = 1, 2, \cdots\cdots, k = \text{number of false targets}, \tag{34}$$

where $\Delta r_{\mathrm{ft},i} = r_{\mathrm{ft},i} - r_j$ or $r_{\mathrm{ft},i} = r_j + \Delta r_{\mathrm{ft},i}$, while $\Delta\tau_{\mathrm{ft},i}$, $\Delta r_{\mathrm{ft},i}$, $r_{\mathrm{ft},i}$, and r_j represent new deceptive time delay increment, deceptive range increment relative to FTG, range of false targets relative to enemy radar, and reference range between enemy radar and jammer, respectively. Hence, the new updated signal will become as follows.

$$y_{\mathrm{ft},i} = \exp\left\{j2\pi f_n\left(\tau_{\mathrm{FTG}}-\tau_{j,m,n}-\Delta\tau_{\mathrm{ft},i}\right)\right\}. \tag{35}$$

Before the transmission of the signal towards the enemy radar, it must undergo carrier modulation with locally generated adjustable carrier frequency. After modulation, signal will be thrown to the enemy radar.

$$\begin{aligned}y_{\mathrm{ft},i}(\mathrm{t}) &= \exp\left\{j2\pi f_n\left(\tau_{\mathrm{FTG}}-\tau_{j,m,n}-\Delta\tau_{\mathrm{ft},i}\right)\right\}\times\exp\left\{j2\pi f_n(t-\Delta\tau_{\mathrm{ft},i})\right\},\\ &= \exp\left\{j2\pi f_n\left(\tau_{FTG}-\tau_{j,m,n}-\Delta\tau_{\mathrm{ft},i}+t-\Delta\tau_{\mathrm{ft},i}\right)\right\},\\ &= \exp\left\{j2\pi f_n\left(t+\tau_{FTG}-\tau_{j,m,n}-2\Delta\tau_{\mathrm{ft},i}\right)\right\}.\end{aligned} \tag{36}$$

The signal received by the enemy radar is

$$\begin{aligned}y_{\mathrm{ft},i,m,n}\left(\mathrm{t}-\tau_{\mathrm{j,m,n}}\right) &= \exp\left\{j2\pi f_n\left(t+\tau_{\mathrm{FTG}}-\tau_{j,m,n}-2\Delta\tau_{\mathrm{ft},i}-\tau_{j,m,n}\right)\right\},\\ &= \exp\left\{j2\pi f_n\left(t+\tau_{\mathrm{FTG}}-2\tau_{j,m,n}-2\Delta\tau_{\mathrm{ft},i}\right)\right\}.\end{aligned} \tag{37}$$

After passing this signal through the matched filter, we get

$$\begin{aligned}y_{\mathrm{ft},i,m,n} &= \exp\left\{j2\pi f_n\left(t+\tau_{\mathrm{FTG}}-2\tau_{j,m,n}-2\Delta\tau_{\mathrm{ft},i}\right)\right\}\times\exp\left\{-\mathrm{j}2\pi\mathrm{f_n}t\right\},\\ &= \exp\left\{j2\pi f_n\left(\tau_{\mathrm{FTG}}-2\tau_{j,m,n}-2\Delta\tau_{\mathrm{ft},i}\right)\right\}.\end{aligned} \tag{38}$$

Now, place values of $\tau_{j,m,n}$ and $\Delta\tau_{\mathrm{ft},i}$, and the received signal will become as

$$\begin{aligned}y_{\mathrm{ft},i,m,n} &= \exp\left\{j2\pi f_n\left(\tau_{\mathrm{FTG}}-2\left[\tau_j-\tau_{j,n}+\tau_{j,m}\right]-2\frac{2\Delta r_{\mathrm{ft},i}}{c}\right)\right\},\\ &= \exp\left\{j2\pi f_n\left(\tau_{\mathrm{FTG}}-\frac{2}{\mathrm{c}}\left[r_j-(n-1)d\sin\theta_j\right.\right.\right.\\ &\qquad\left.\left.\left.+(m-1)d\sin\theta_j\right]-\frac{4}{c}\left[r_{\mathrm{ft},i}-r_j\right]\right)\right\}.\end{aligned} \tag{39}$$

As we know that $f_n = f_0 + (n-1)\Delta f$,

$$\begin{aligned}y_{\mathrm{ft},i,m,n} &= \exp\left\{j2\pi(f_0+(n-1)\Delta f)\begin{bmatrix}\tau_{\mathrm{FTG}}-\frac{2\mathrm{r_j}}{\mathrm{c}}+\frac{2(n-1)d\sin\theta_j}{c}\\ -\frac{2(m-1)d\sin\theta_j}{c}-\frac{4r_{\mathrm{ft},i}}{c}+\frac{4r_j}{c}\end{bmatrix}\right\},\\ &= \exp\left\{j2\pi(f_0+(n-1)\Delta f)\left[\tau_{\mathrm{FTG}}+\frac{2\mathrm{r_j}}{\mathrm{c}}+\frac{2(n-1)dsin\theta_j}{c}-\frac{2(m-1)dsin\theta_j}{c}-\frac{4r_{\mathrm{ft},i}}{c}\right]\right\},\\ &= \exp\left\{j2\pi\begin{bmatrix}f_0\tau_{\mathrm{FTG}}+f_0\frac{2\mathrm{r_j}}{\mathrm{c}}+\frac{2(n-1)f_0d\sin\theta_j}{c}-\frac{2(m-1)f_0d\sin\theta_j}{c}\\ -\frac{4f_0r_{\mathrm{ft},i}}{c}+(n-1)\Delta f\tau_{\mathrm{FTG}}+\frac{2(n-1)\Delta f\mathrm{r_j}}{\mathrm{c}}+\frac{2(n-1)^2\Delta fd\sin\theta_j}{c}\\ -\frac{2(n-1)(m-1)\Delta fd\sin\theta_j}{c}-\frac{4(n-1)\Delta fr_{\mathrm{ft},i}}{c}\end{bmatrix}\right\}.\end{aligned} \tag{40}$$

Terms I and II will be taken outside, while terms VI, VIII, and IX will be ignored due to their insignificance.

$$y_{\mathrm{ft},i,m} = \exp\{\mathrm{j}2\pi f_0 \tau_{\mathrm{FTG}}\} \times \exp\left\{\mathrm{j}4\pi \frac{f_0 \mathrm{r_j}}{\mathrm{c}}\right\} \sum_{n=1}^{N} \exp\left\{ j2\pi \left[\begin{array}{l} \frac{2(n-1)f_0 d \sin\theta_j}{c} - \\ \frac{2(m-1)f_0 d \sin\theta_j}{c} - \frac{4f_0 r_{\mathrm{ft},i}}{c} + \\ \frac{2(n-1)\Delta f \mathrm{r_j}}{\mathrm{c}} - \frac{4(n-1)\Delta f r_{\mathrm{ft},i}}{c} \end{array} \right] \right\},$$
$$= \mathrm{A}_\varphi \sum_{n=1}^{N} \exp\left\{ \frac{j4\pi}{c} \left[\begin{array}{l} (n-1)f_0 d \sin\theta_j - (m-1)f_0 d \sin\theta_j \\ -2f_0 r_{\mathrm{ft},i} + (n-1)\Delta f \mathrm{r_j} - 2(n-1)\Delta f r_{\mathrm{ft},i} \end{array} \right] \right\}, \tag{41}$$

where $\mathrm{A}_\varphi = \exp\{\mathrm{j}2\pi f_0 \tau_{\mathrm{FTG}}\} \times \exp\{\mathrm{j}4\pi(f_0 \mathrm{r_j}/\mathrm{c})\}$ represents the phase change due to the enemy radar to jammer reference distance and time due to signal interception and processing time delay. For simplicity, we can ignore A_φ.

$$y_{\mathrm{ft},i,m,n} = \exp\left\{ j4\pi \left[\begin{array}{l} \frac{(n-1)f_0 d \sin\theta_j}{c} - \frac{(m-1)f_0 d \sin\theta_j}{c} \\ -\frac{2f_0 r_{\mathrm{ft},i}}{\mathrm{c}} + \frac{(n-1)\Delta f \mathrm{r_j}}{c} - \frac{2(n-1)\Delta f r_{\mathrm{ft},i}}{c} \end{array} \right] \right\}. \tag{42}$$

Now, we can deform above result into two factors: direction and range.

$$y_{\mathrm{ft},i,m,n} = \exp\left\{ -j4\pi \left[\begin{array}{l} \left(\frac{(n-1)f_0 d \sin\theta_j}{c} - \frac{(m-1)f_0 d \sin\theta_j}{c}\right) \\ \times \left(\frac{2f_0 r_{\mathrm{ft},i}}{\mathrm{c}} + \frac{2(n-1)\Delta f r_{\mathrm{ft},i}}{c} - \frac{(n-1)\Delta f \mathrm{r_j}}{c}\right) \end{array} \right] \right\}. \tag{43}$$

For the sake of simplicity, we can ignore the 1st factor which represents radiation pattern due to direction, and we consider only the 2nd factor here which is our current area of discussion.

$$y_{\mathrm{ft},i,m,n} = \exp\left\{ -j4\pi \left[\frac{2f_0 r_{\mathrm{ft},i}}{\mathrm{c}} + \frac{2(n-1)\Delta f r_{\mathrm{ft},i}}{c} - \frac{(n-1)\Delta f \mathrm{r_j}}{c} \right] \right\}. \tag{44}$$

Now, we have these three terms which are range-dependent and playing important role of determining the radiation pattern of the desired signal. It is evident that first and second terms are representing fake target ranges while third term is representing actual target range. Third term is the most insignificant term as relative to other contributing terms, and due to this reason, its effect will be overcome by other terms, or it can be simply ignored.

$$y_{\mathrm{ft},i,m,n} = \exp\left\{ -j4\pi \left[\frac{2f_0 r_{\mathrm{ft},i}}{\mathrm{c}} + \frac{2(n-1)\Delta f r_{\mathrm{ft},i}}{c} \right] \right\}. \tag{45}$$

Hence, the enemy radar will observe the fake targets rather than observing the actual target.

Table 1: Parameters of actual and false targets.

Case#	Parameter	Actual target	FT 1	FT 2	FT 3	FT 4
1	Range (km)	50	30	40	60	70
	Angle (degrees)	50	50	50	50	50
2	Range (km)	40	30	50	60	70
	Angle (degrees)	10	10	10	10	10
3	Range (km)	70	40	50	60	80
	Angle (degrees)	40	40	40	40	40
4	Range (km)	60	40	50	70	80
	Angle (degrees)	20	20	20	20	20

5. Simulations

Our objective in this simulation is to offer deception jamming to the enemy radars. Consider the proposed scenario as shown in Figure 5 which is based on the surface to the air signal model. The actual aircraft is situated in air far-zone field while the opponent FDA radar is located at the surface. The proposed deceptive jammer is mounted on the actual aircraft. Both rivals are working on W-band ($f_0 = 100\ GHz$) of the FDA radar having N number of isotropic antenna elements with equal interelement spacing $\lambda/2$ and uniform current distribution along the whole linear array geometry configuration. The frequency increment of the FDA radars is kept$\Delta f = 0.3$ KHz.

Our proposed deceptive jammer works in passive searching mode that means it does not transmit and receive own signals to scan opponent radar. It instead utilizes the opponent radar signals to trace the desired parameters. But as quick as the computational system at the target finds direction of arrival (DOA), range, and pulse repetition interval (PRI) of the opponent radar, our proposed method can send deceptive echoes towards the opponent radar. These deceptive-echoes carry radiation pattern with appropriate null linked to the desired range and direction. They will be transmitted back in synchronous with actual target echoes to hide the actual target and delayed versions of false echoes to generate multiple false targets. Afterwards, in result of the proposed algorithm, the opponent radar will not be able to navigate the actual aircraft. So, track mode of the opponent radar will not work here.

To avoid any waveform time-dependent periodicity and mutual interference between the array element pulse width of the echo that is kept $\leq 30\ \mu s$ and for the sake of simplicity, the PRI is taken 0.5 ms. Four different simulation cases have been considered. In each case, one true target is assumed, and the proposed deceptive jammer is mounted on it. The technique hides the actual aircraft along with generating four false targets in each test case with the parameters given in Table 1. For 3-D simulations, ten radiating antenna elements are considered, but for the 2-D simulations, we have taken $N = 10, 20, 30, 40, 50$ isotropic antenna elements, in the ULA-based FDA radar for each case.

6. Case-I

In first case, we assume that the actual target aircraft is situated at distance 50 km and direction 50 degrees. Frequency

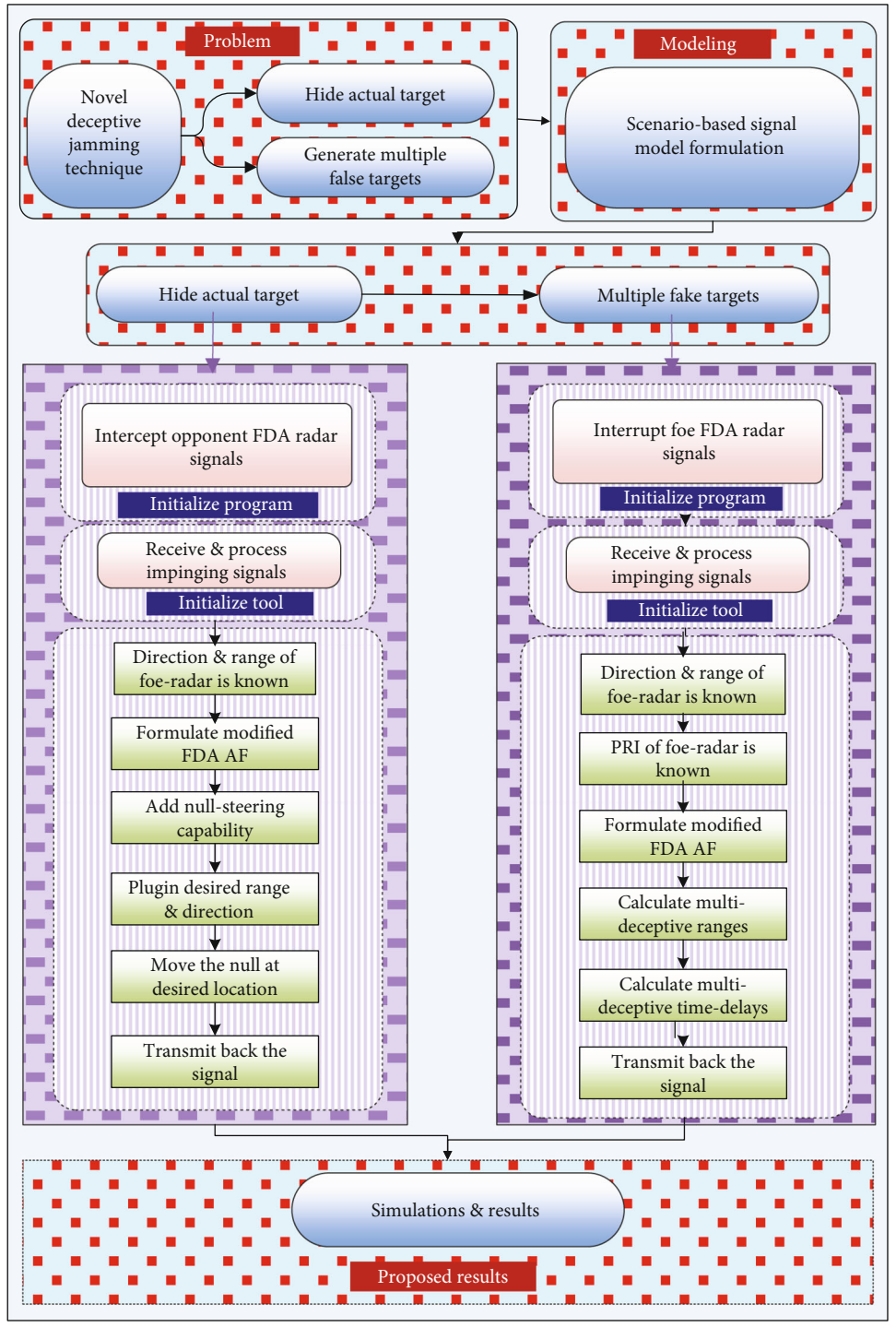

Figure 6: Proposed model.

of the first element in the array is taken 100 GHz, while incremental frequency is assumed 0.3 kHz. Figure 7 shows 3-D simulation of the case where null has been placed at the real target aircraft location in order to hide it from the enemy radar. We have considered different numbers of antenna-elements in the array of ULA-based FDA radar for 2-D simulations.

Instead of showing results like Figures 7, 11, 15, and 19 in 3-D, we have plotted the results in more simplified way using only output power in Figures 10, 14, 18, and 22, respectively. These figures (10, 14, 18, and 22) simply further elaborate the results of Figures 7, 11, 15, and 19, respectively. These figures show two scenarios. In the first scenario, it hides the actual target by simulating equation (29), whereas eq. (29) places null in the received signal at the opponent radar's location by means when the opponent receives this signals, he will perceive min. power at the target location. In the second scenario, it generates false targets at certain ranges and angles by

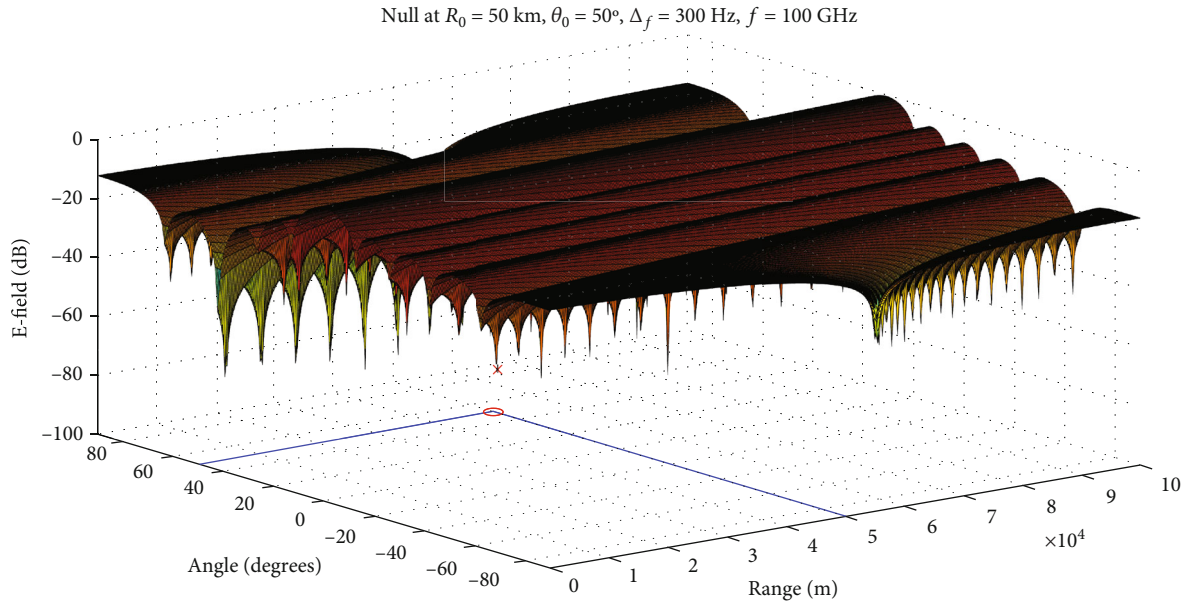

Figure 7: Actual target hides at distance 50 km and direction 50°.

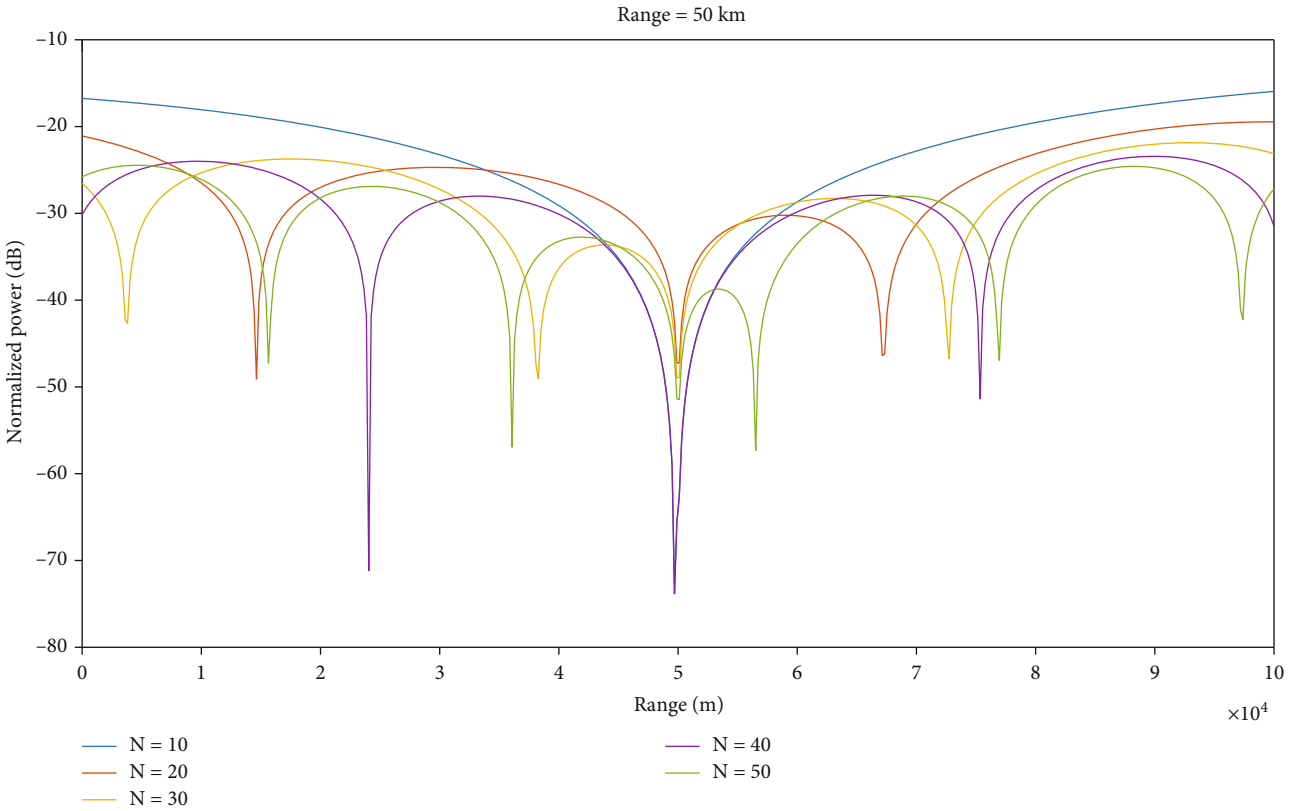

Figure 8: Null's placement at opponent radar's range with different numbers of antenna elements.

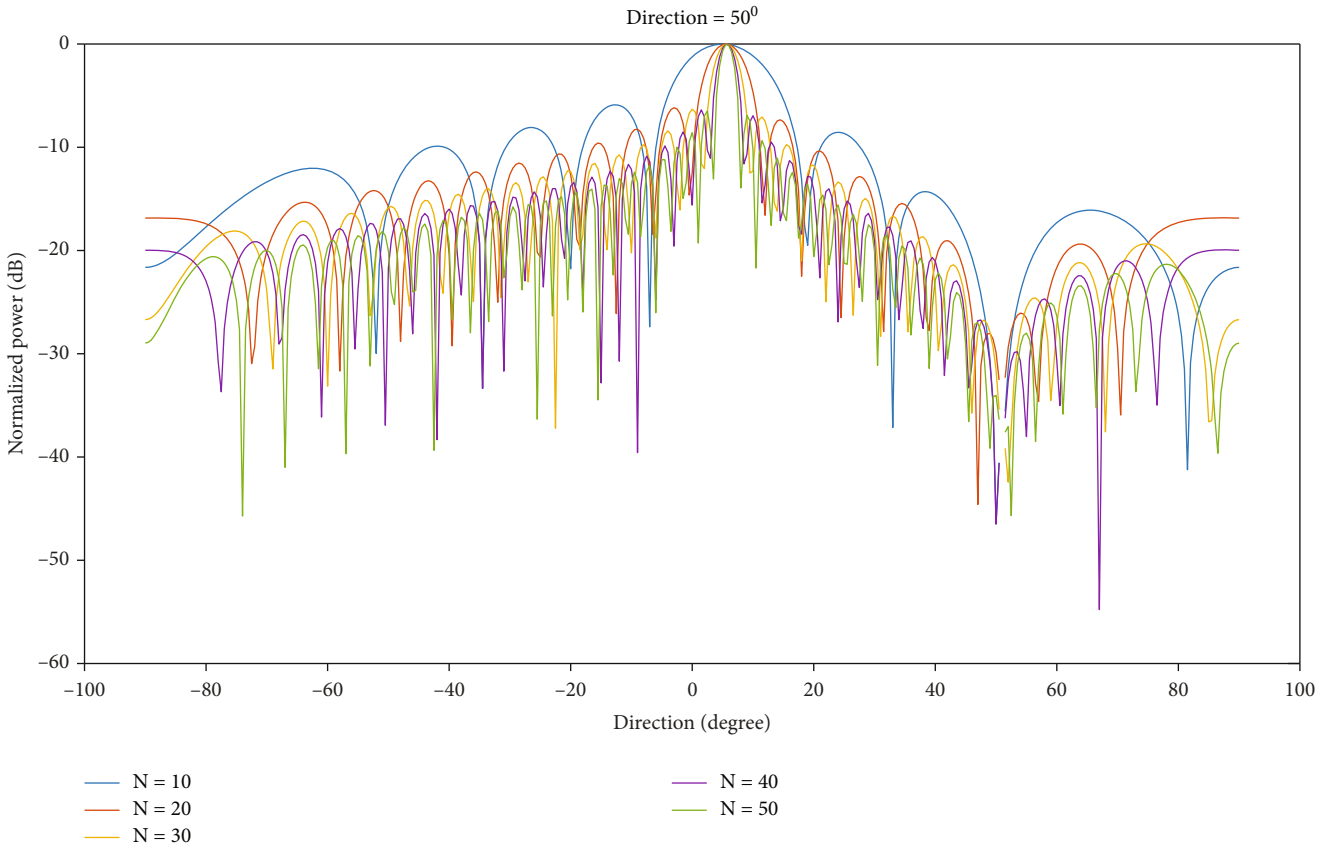

Figure 9: Null's placement at opponent radar's direction with different numbers of antenna elements.

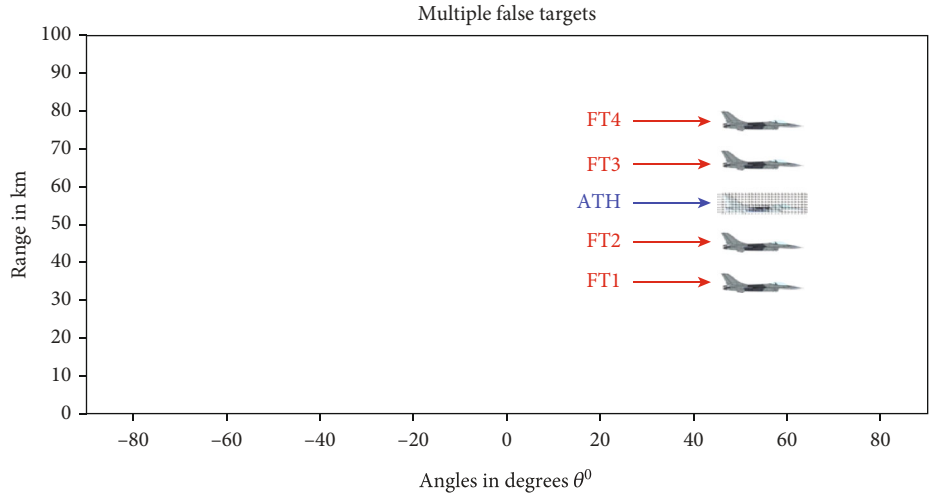

Figure 10: Actual target hides at 50 km, and false targets appear at {30, 40, 60, 70} km.

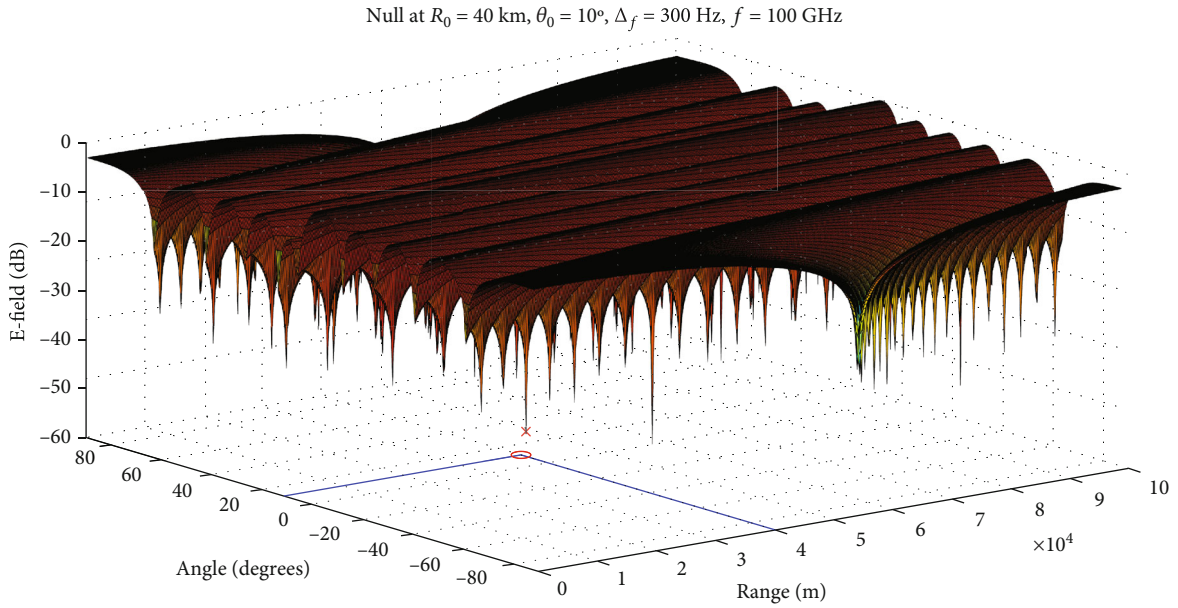

Figure 11: Actual target hides at distance 40 km and direction 10°.

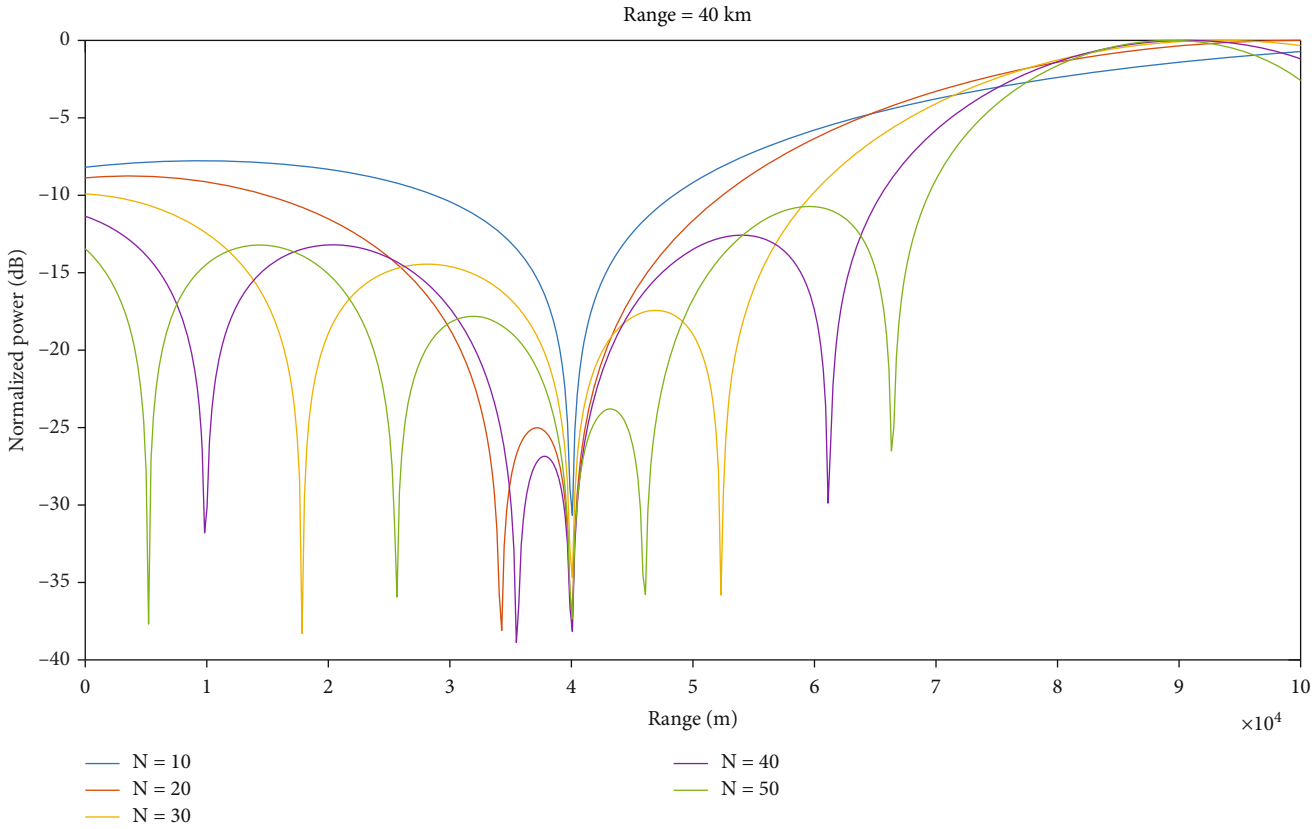

Figure 12: Null's placement at opponent radar's range with different numbers of antenna elements.

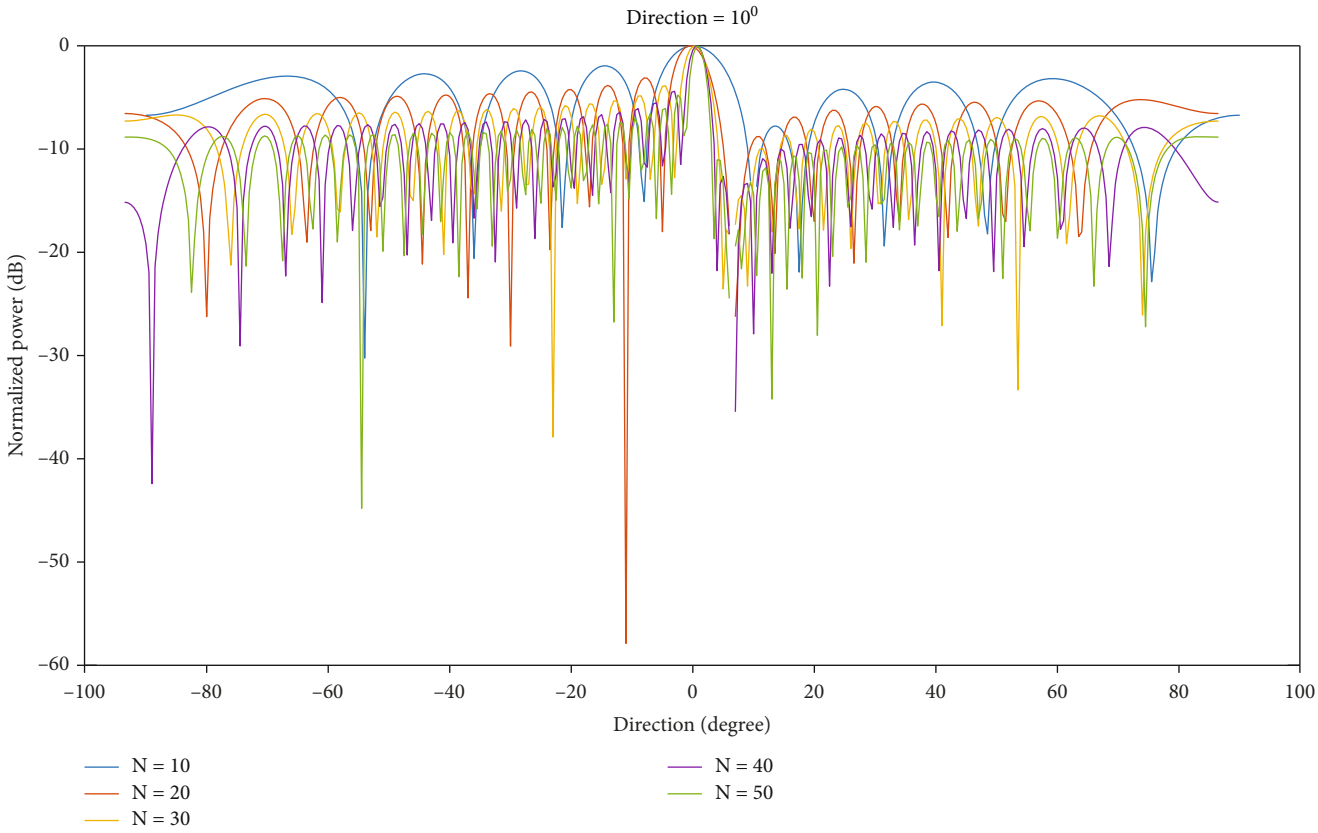

Figure 13: Null's placement at opponent radar's direction with different numbers of antenna elements.

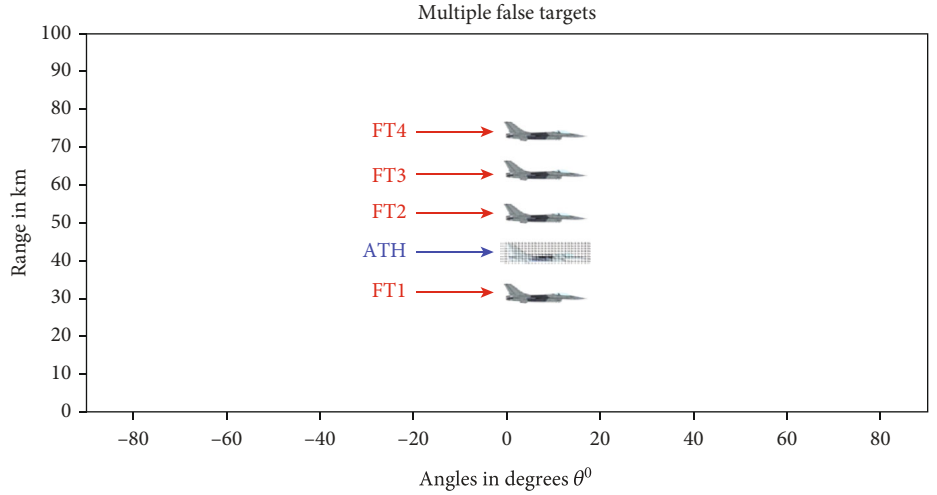

Figure 14: Actual target hides at 40 km, and false targets appear at {30, 50, 60, 70} km.

evaluating equation (45) which will offer maximum power at different ranges.

Figure 8 reflects 2-D results of the null position at the range of the actual aircraft to camouflage it, while Figure 9 also verifies our results of null position at the desired direction of the real target to cover it. The proposed method also generates four fake targets along the same direction of the actual target and at different ranges of 30 km, 40 km, 60 km, and 70 km. This has been proved in Figure 10 where the desired target is hidden along with fake targets at their respective ranges.

7. Case-II

For this case, we have assumed that the real-target aircraft is located at range 40 km and direction 10 degree. Carrier frequency and incremental frequency, f_0 and Δf, are considered 100 GHz and 0.3 kHz, respectively. Figure 11 represents a 3-

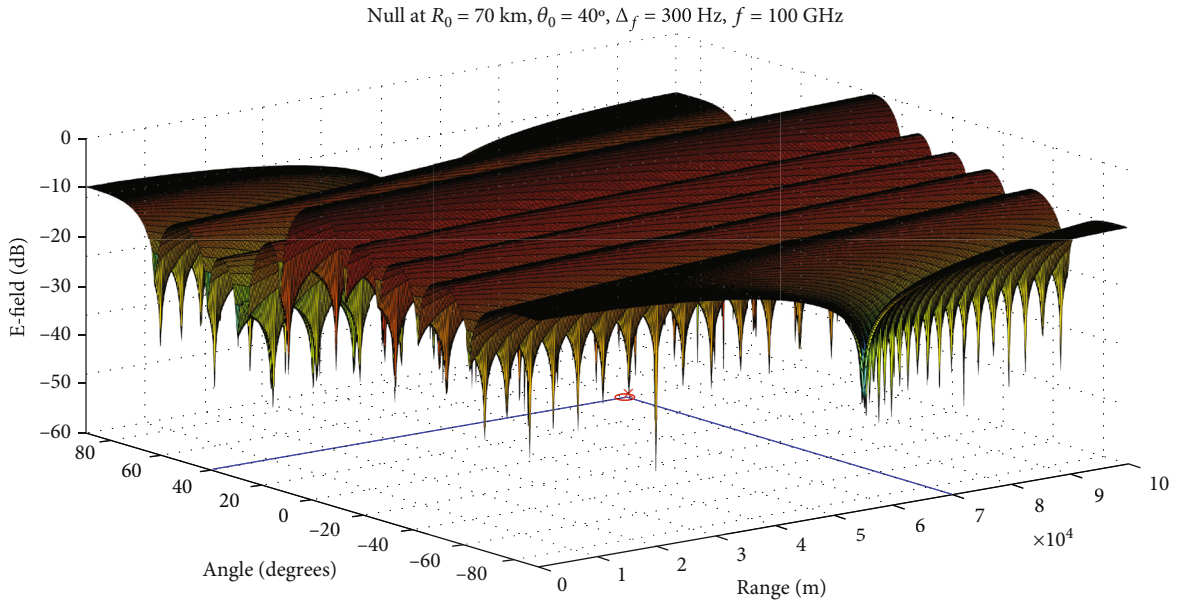

Figure 15: Actual target hides at distance 70 km and direction 40°.

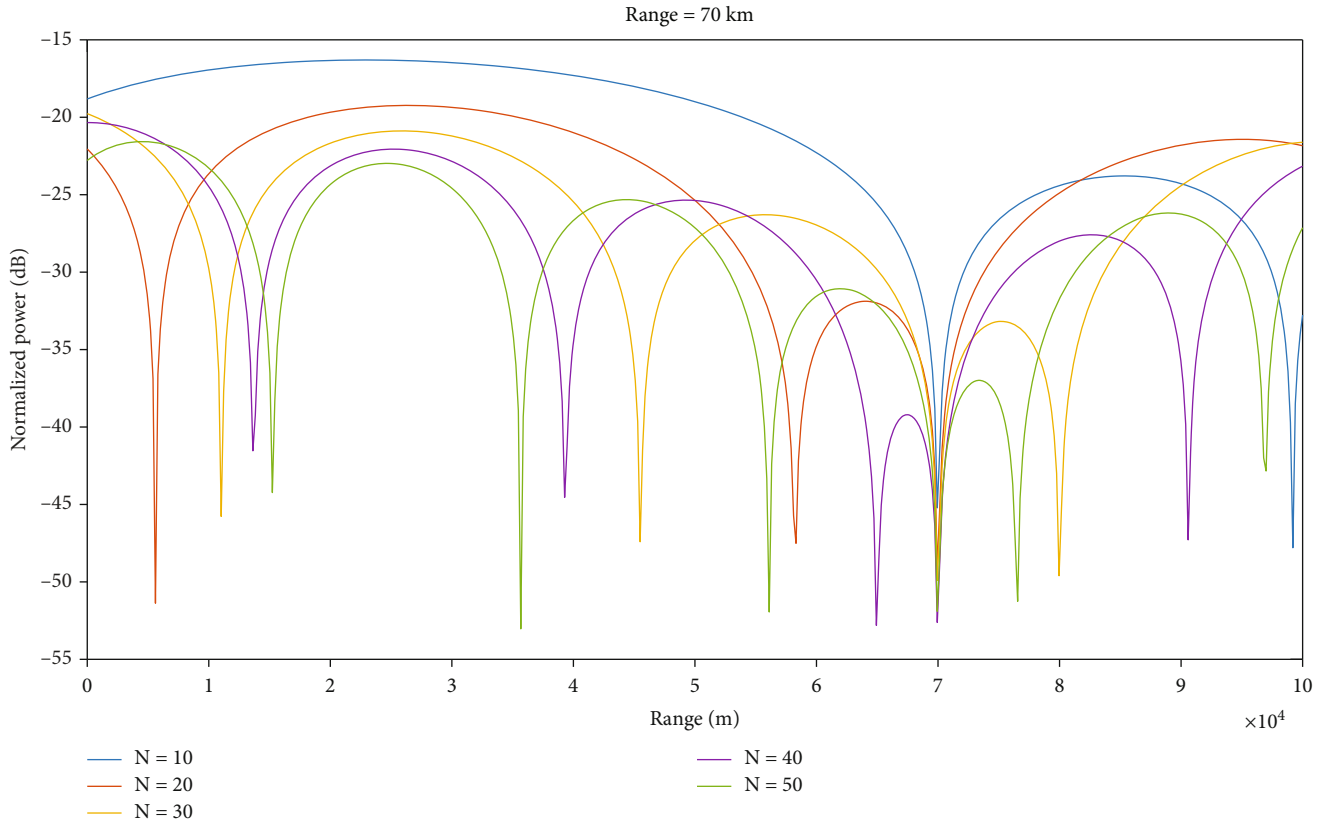

Figure 16: Null's placement at opponent radar's range with different numbers of antenna elements.

D simulation where the desired null has been placed at the real target aircraft location to hide it from the opponent radar. Two-dimensional results of the null position at the desired range (40 km) of the actual-aircraft are shown in Figure 12. In another graph, we have proved that the null has been placed at the desired direction of the actual target aircraft reflected in Figure 13. Further, our technique also generates four false targets along the direction 10 degrees but at ranges of 30 km, 50 km, 60 km, and 70 km as shown in Figure 14.

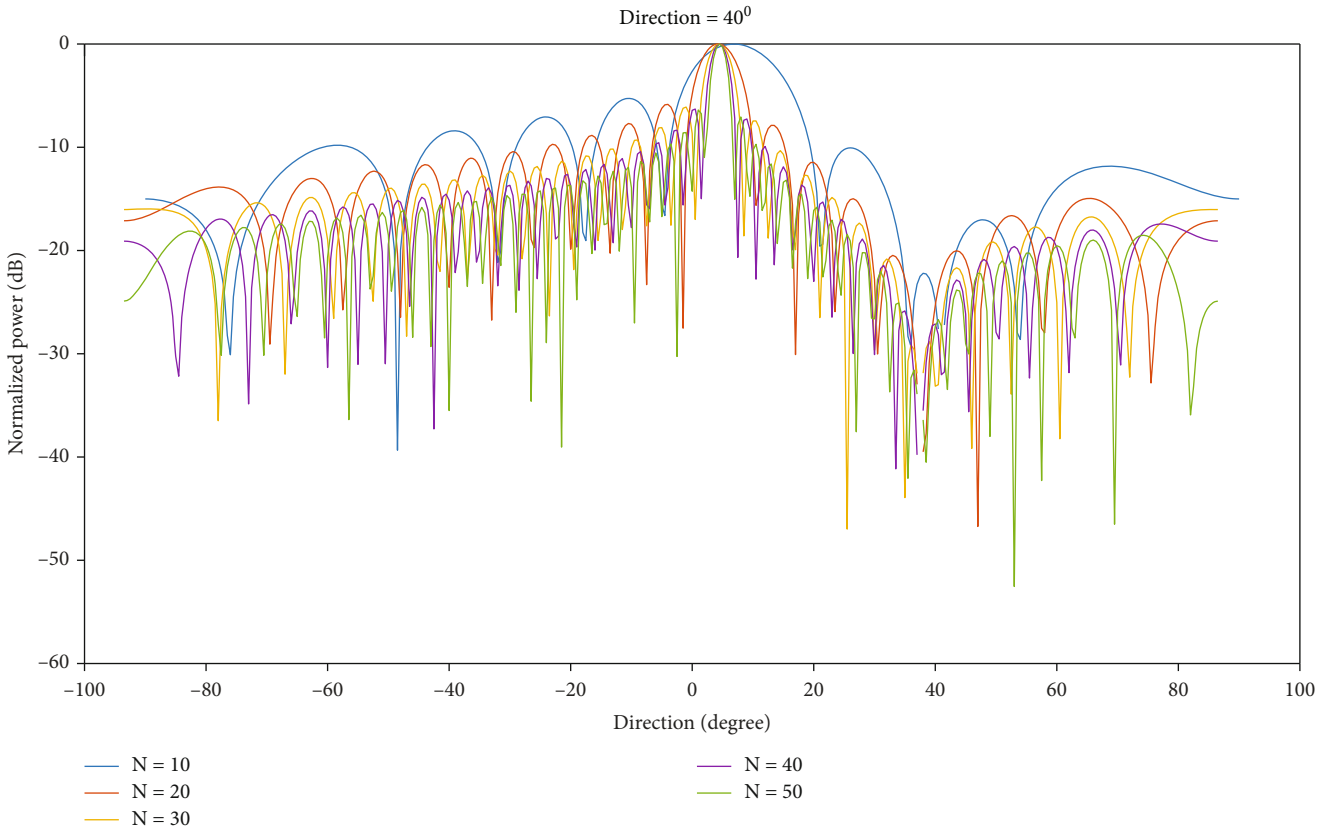

Figure 17: Null's placement at opponent radar's direction with different numbers of antenna elements.

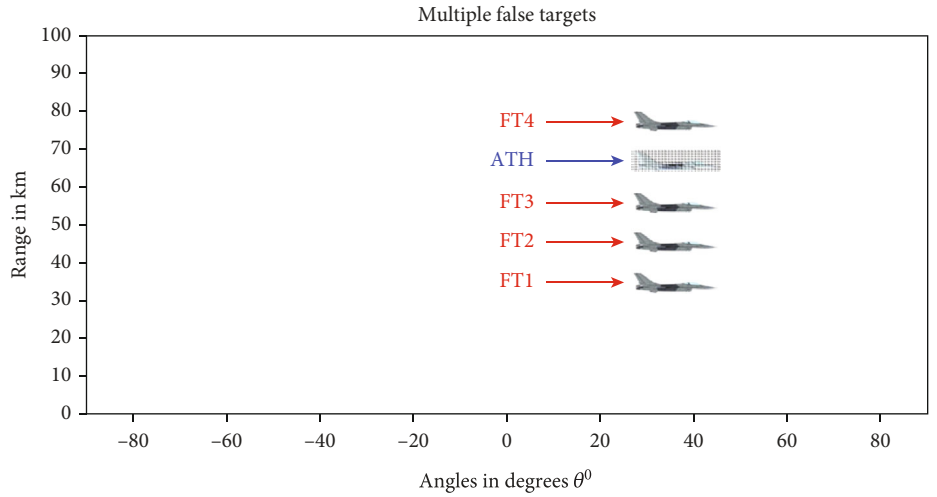

Figure 18: Actual target hides at 70 km, and false targets appear at {40, 50, 60, 80} km.

8. Case-III

In 3rd case, we have assumed that the real target is positioned at range of 70 km from the opponent radar along the direction 40 degrees. Our proposed technique can verify the results in Figure 15 by showing that the desired null has been place effectively at the actual target location. Its two-dimensional counterpart graphs are shown in Figures 16 and 17 to validate its correctness in the desired range and direction, respectively. Figure 18 shows multiple fake targets in the direction of the real target but at distances 40 km, 50 km, 60 km, and 80 km away from the opponent radar.

9. Case-IV

In the last case, we have taken the actual target aircraft at distance 60 km away from the foe radar and at direction 20 degrees. The proposed model draws a null at its location to

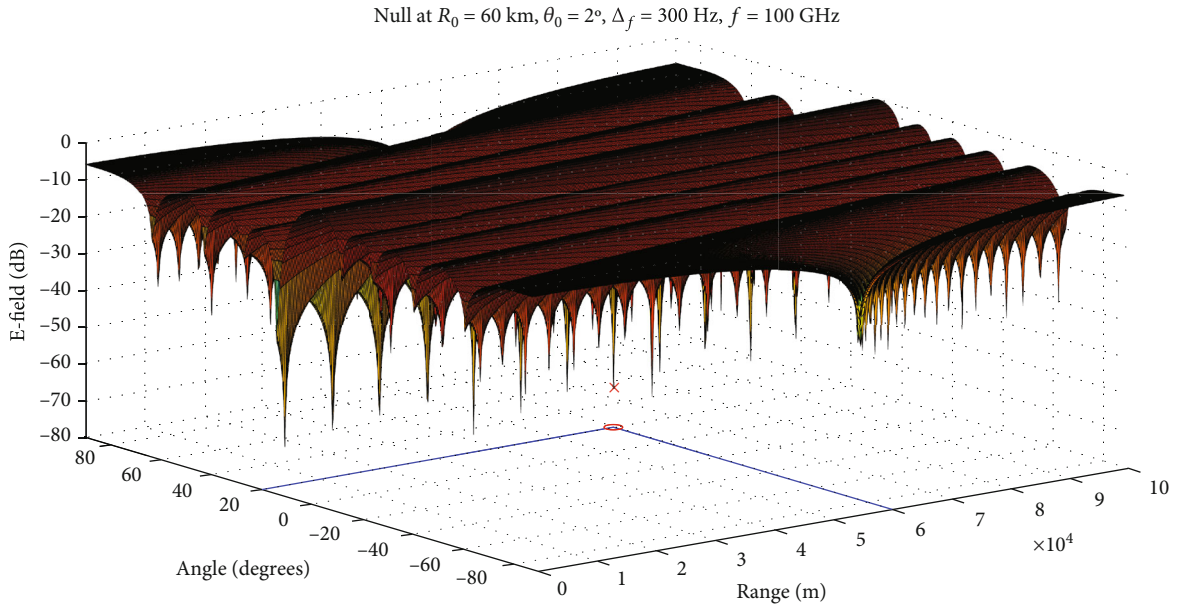

Figure 19: Actual target hides at distance 60 km and direction 20°.

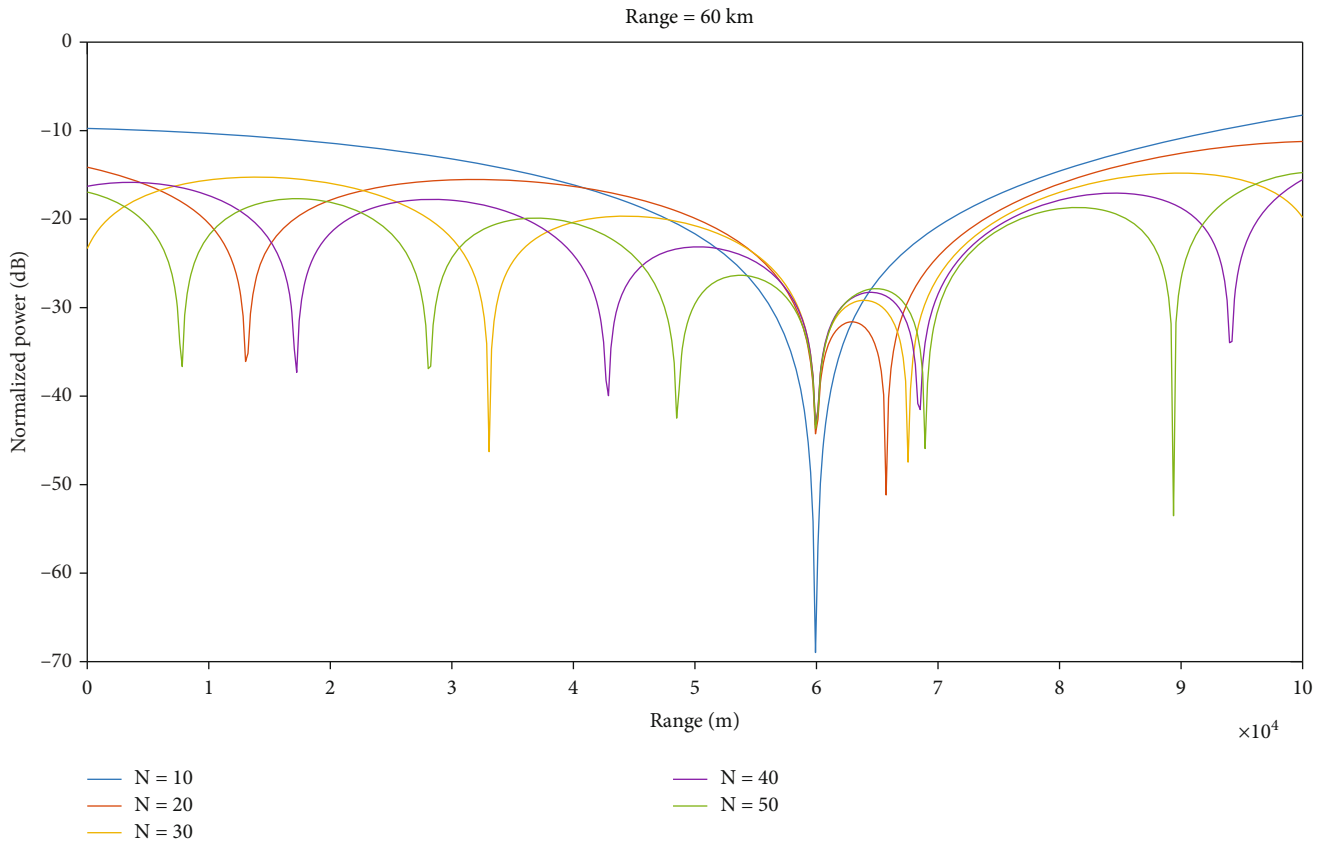

Figure 20: Null's placement at opponent radar's range with different numbers of antenna elements.

hide the aircraft from the vision of the opponent radar, and it is evident from its 3-D simulation in Figure 19. Further exploration of the method has been disclosed in Figures 20 and 21, whereby 2-dimensional graphs have been drawn to show the placement of the null at the desired range and direction, respectively. Vertical axis shows power in dB for different numbers of radiating antenna elements in the array. Lastly, to generate multiple fake targets at range 40 km, 50 km, 70 km, and 80 km along the same direction of the target aircraft, the proposed method calculates appropriate time

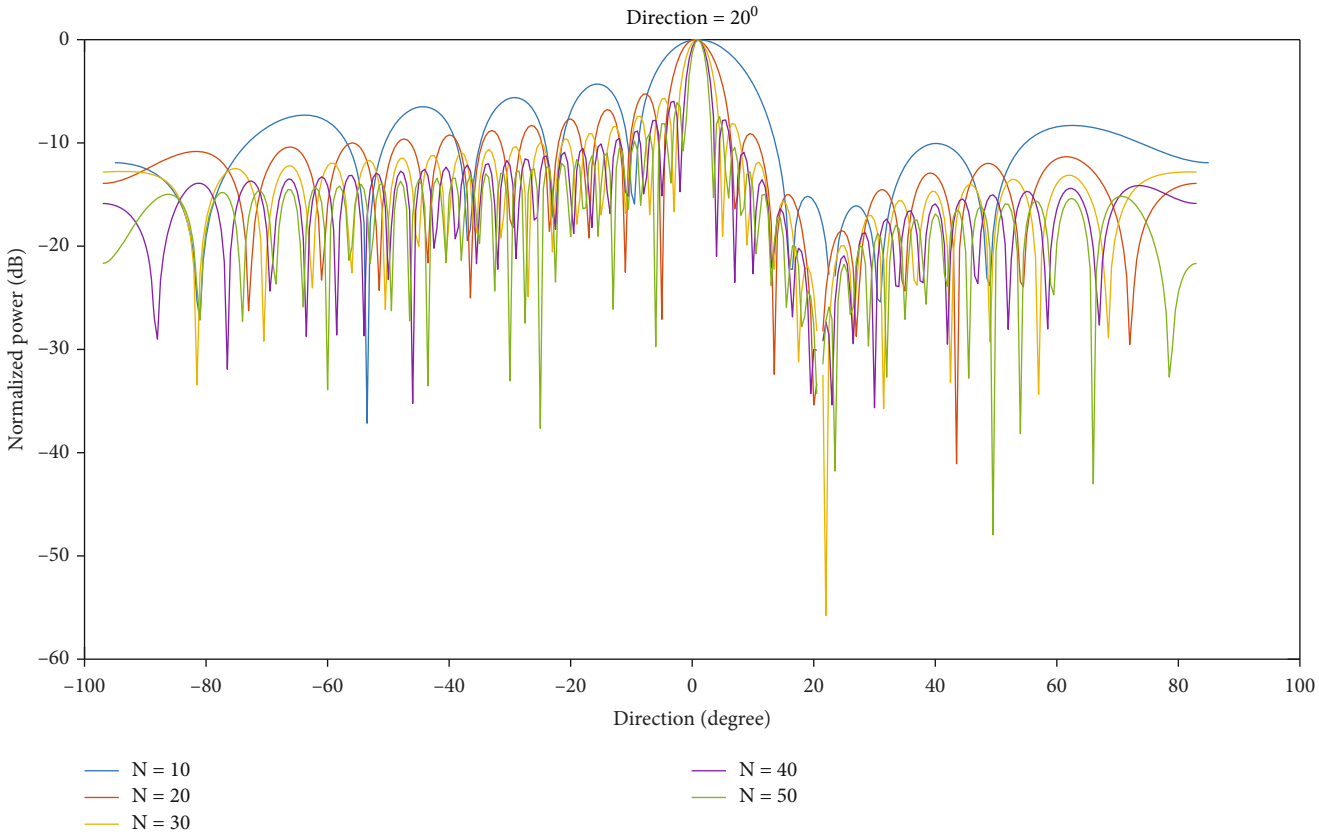

Figure 21: Null's placement at opponent radar's direction with different numbers of antenna elements.

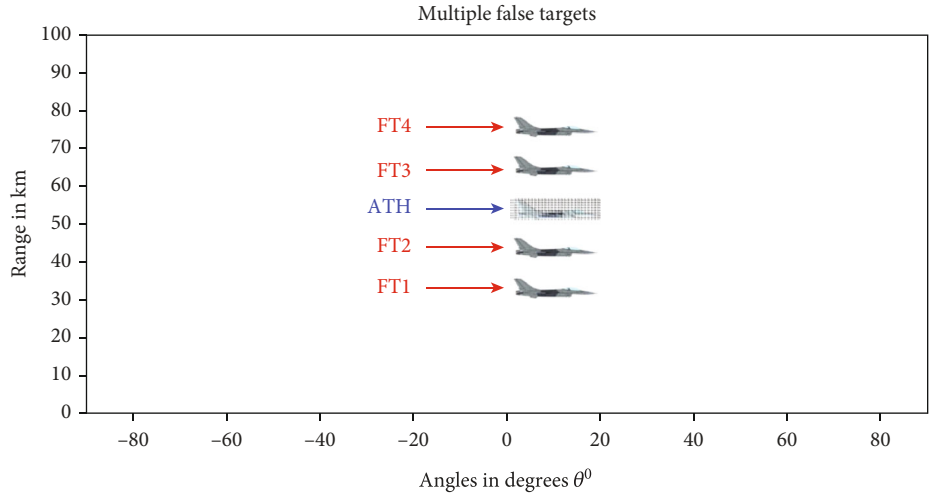

Figure 22: Actual target hides at 60 km, and false targets appear at {40, 50, 70, 80} km.

delays. The deceptive jammer sends echoes back with these time delays to confuse the enemy radar by showing him multiple false targets at desired ranges as shown in Figure 22.

10. Conclusion and Future Directions

A novel approach in the field of deception jamming has been developed in this research which hides actual target and displays multiple fake targets at different arbitrary ranges along the same direction to the enemy radar. This method has been developed to neutralize the effectiveness and dangers of the enemy radar which ultimately guarantees the safe penetration of the actual aircraft into the enemy territory. Moreover, a number of time modulations are performed for intercepted signal to display multiple deceptive jammer false targets at different ranges but along the same direction. It is assumed that the enemy radar has the capability of range angle-dependent radiation pattern characteristics. FDA radar's

radiation pattern is also time-dependent for larger pulse width. This effect has been covered by considering narrow radar pulse width. Hence, in this way, time dependency will not affect the radiation pattern of the FDA radar.

One of the other emerging area of research is how to counter deception jamming (anti-jamming) using FDA-MIMO radars in the field of ECCM techniques, because in the FDA-MIMO radar, we synthesize features of both radars (FDA and MIMO), and we achieve frequency diversity due to the FDA radar as well as waveform diversity due to the MIMO radar. We will try to investigate their relation with the presented method as well. We will also explore that how we can use FDA-MIMO radars to hide the actual aircraft target from the ground-based FDA opponent radar without the help of wave-scattering reflectors or advance escort-free-drone jammer. This research can give notion towards production of airborne deceptive jammers in the future.

Finally, the effectiveness and correctness of the proposed research have been verified by doing theoretical analysis and simulations by considering different cases with a number of distinct ranges of the actual target and fake deceptive targets. To put the research in the simplest form, the FDA radar is considered with the uniform linear array configuration. Moreover, the passage of time hardware computational and accuracy capabilities increases tremendously. Hence, limitations in implementing the algorithms due to hardware will be overcome; one can implement the proposed work through hardware with the collaboration of any national/international research organization.

Data Availability

All the data used in this work is based on simulations in MATLAB and is available for any research work.

Conflicts of Interest

All the authors declare that there is no conflict of interest.

Acknowledgments

Prof. Dr. Ijaz Mansoor Qureshi, a prolific Pakistani scholar, engineer, and scientist, suddenly died on the 10th of January 2021 at the age of 67. A renowned expert of signal array processing and evolutionary computing techniques, Professor Qureshi worked in different national universities of Pakistan for decades. He authored more than 200 publications and mentored more than 50 PhD scholars, including myself. Knowledge, wisdom, and experience in the field were aspects of his life; moreover, he was a man of great hospitality, friendship, and kindness. The authors found him warm, smiling, and engaging. Simplicity and morality were the salient features of his personality. His scholarship, penetrating mind, and truly and lovely personality will be long remembered in our minds and hearts.

References

[1] B. Zohuri, "Electronic countermeasure and electronic counter-countermeasure," in *Radar Energy Warfare and the Challenges of Stealth Technology*, pp. 111–145, Springer, Cham, 2020.

[2] Y. Yan-Juan, Z. Feng, A. Xiao-Feng, L. Xiao-Bin, and Z.-F. Xu, "A study on effectiveness modeling of multi-false-target jamming," in *2016 CIE International Conference on Radar (RADAR)*, pp. 1–5, Guangzhou, China, 2016.

[3] A. Farina and M. Skolnik, "Electronic counter-countermeasures," *Radar handbook 2*, McGraw-Hill Education, 2008.

[4] L. Neng-Jing and Z. Yi-Ting, "A survey of radar ECM and ECCM," *IEEE Transactions on Aerospace and Electronic Systems*, vol. 31, no. 3, pp. 1110–1120, 1995.

[5] A. Ahmed, W. Q. Wang, Z. Yuan, S. Mohamed, and T. Bin, "Subarray-based FDA radar to counteract deceptive ECM signals," *EURASIP Journal on Advances in Signal Processing*, vol. 2016, no. 1, 2016.

[6] S. Y. Nusenu, A. Basit, and E. Asare, "FDA transmit beamforming synthesis using Chebyshev window function technique to counteract deceptive electronic countermeasures signals," *Progress in Electromagnetics Research Letters*, vol. 90, pp. 53–60, 2020.

[7] F. H. Zhao, P. Zhang, and Y. S. Wang, "The study of barrage-type jamming for SAR," *Wireless Communication Technology*, vol. 16, no. 3, pp. 53–57, 2007.

[8] J. Schuerger and D. Garmatyuk, "Deception jamming modeling in radar sensor networks," in *MILCOM 2008 - 2008 IEEE Military Communications Conference*, pp. 1–7, San Diego, CA, USA, 2008.

[9] Y. Li, L. Gaohuan, and C. Huilian, "The study of multi-false targets deception against stepped-frequency waveform inverse synthetic aperture radar," in *2008 9th International Conference on Signal Processing*, pp. 2481–2484, Beijing, China, 2008.

[10] Y. J. Lee, J. R. Park, W. H. Shin, K. I. Lee, and H. C. Kang, "A study on jamming performance evaluation of noise and deception jammer against SAR satellite," in *2011 3rd International Asia-Pacific Conference on Synthetic Aperture Radar (APSAR)*, pp. 1–3, Seoul, Korea (South), 2011.

[11] B. Rao, G. Zhaoyu, and Y. Nie, "Deception approach to track-to-track radar fusion using noncoherent dual-source jamming," *IEEE Access*, vol. 8, pp. 50843–50858, 2020.

[12] S. ZHU, Q. Luo, and C. Tong, "The analysis of moving targets deceptive jamming model to SAR," *Electronic Information Warfare Technology*, vol. 1, p. 13, 2012.

[13] F. Zhou, B. Zhao, M. Tao, X. Bai, B. Chen, and G. Sun, "A large scene deceptive jamming method for space-borne SAR," *IEEE Transactions on Geoscience and Remote Sensing*, vol. 51, no. 8, pp. 4486–4495, 2013.

[14] B. Zhao, F. Zhou, M. Tao, Z. Zhang, and B. Zheng, "Improved method for synthetic aperture radar scattered wave deception jamming," *IET Radar, Sonar & Navigation*, vol. 8, no. 8, pp. 971–976, 2014.

[15] Y. Liu, W. Wang, X. Pan, D. Dai, and D. Feng, "A frequency-domain three-stage algorithm for active deception jamming against synthetic aperture radar," *IET Radar, Sonar & Navigation*, vol. 8, no. 6, pp. 639–646, 2014.

[16] X. Yan, Y. Li, P. Li, and J. Wang, "Multiple time-delay smart deception jamming to pseudo-random code phase modulation fuze," in *2012 International Conference on Computer*

Distributed Control and Intelligent Environmental Monitoring, pp. 428–432, Zhangjiajie, China, 2012.

[17] P. Shi-rui, L. Yong-chun, L. Xin, and W.-f. Dong, "Study on target pose and deception jamming to ISAR," in *2009 2nd Asian-Pacific Conference on Synthetic Aperture Radar*, pp. 526–530, Xi'an, China, 2009.

[18] Z. Zong, L. Huang, H. Wang, L. Huang, and Z. Shu, "Micro-motion deception jamming on Sar using frequency diverse array," in *IGARSS 2019 - 2019 IEEE International Geoscience and Remote Sensing Symposium*, pp. 2391–2394, Yokohama, Japan, 2019.

[19] Z. Bo, F. Zhou, X. Shi, Q. Wu, and Z. Bao, "Multiple targets deception jamming against ISAR using electromagnetic properties," *IEEE Sensors Journal*, vol. 15, no. 4, pp. 2031–2038, 2014.

[20] W. Wang, X.-Y. Pan, Y.-C. Liu, D.-J. Feng, and F. Qi-Xiang, "Sub-Nyquist sampling jamming against ISAR with compressive sensing," *IEEE Sensors Journal*, vol. 14, no. 9, pp. 3131–3136, 2014.

[21] X.-Y. Pan, W. Wang, and G.-Y. Wang, "Sub-Nyquist sampling jamming against ISAR with CS-based HRRP reconstruction," *IEEE Sensors Journal*, vol. 16, no. 6, pp. 1597–1602, 2015.

[22] L. X. D. Feng, Q. Liu, and X. Wang, "ISAR decoy generation by utilizing coherent multiplication modulated jamming," *Acta Electronica Sinica*, vol. 42, no. 12, pp. 2501–2508, 2014.

[23] D. Feng, L. Xu, X. Pan, and X. Wang, "Jamming wideband radar using interrupted-sampling repeater," *IEEE Transactions on Aerospace and Electronic Systems*, vol. 53, no. 3, pp. 1341–1354, 2017.

[24] Q. Shi, C. Wang, J. Huang, and N. Yuan, "Multiple targets deception jamming against ISAR based on periodic 0- π phase modulation," *IEEE Access*, vol. 6, pp. 3539–3548, 2018.

[25] P. Antonik, M. C. Wicks, H. D. Griffiths, and C. J. Baker, "Frequency diverse array radars," in *2006 IEEE Conference on Radar*, p. 3, Verona, NY, USA, 2006.

[26] P. Antonik, M. C. Wicks, H. D. Griffiths, and C. J. Baker, "Multi-mission multi-mode waveform diversity," in *2006 IEEE Conference on Radar*, p. 3, Verona, NY, USA, 2006.

[27] P. Antonik and M. C. Wicks, "Method and apparatus for simultaneous synthetic aperture radar and moving target indication," US Patent 8,803,732, 2014.

[28] P. Antonik, M. C. Wicks, H. D. Griffiths, and C. J. Baker, "Range-dependent beamforming using element level waveform diversity," in *2006 International Waveform Diversity & Design Conference*, pp. 1–6, Lihue, HI, USA, 2006.

[29] M. Secmen, S. Demir, A. Hizal, and T. Eker, "Frequency diverse array antenna with periodic time modulated pattern in range and angle," in *2007 IEEE Radar Conference*, pp. 427–430, Waltham, MA, USA, 2007.

[30] P. F. Sammartino, C. J. Baker, and H. D. Griffiths, "Frequency diverse MIMO techniques for radarIEEE Transactions on Aerospace and Electronic Systems," vol. 49, no. 1, pp. 201–222, 2013.

[31] W.-Q. Wang, "Range-angle dependent transmit beampattern synthesis for linear frequency diverse arrays," *IEEE Transactions on Antennas and Propagation*, vol. 61, no. 8, pp. 4073–4081, 2013.

[32] W.-Q. Wang, "Frequency diverse array antenna: new opportunities," *IEEE Antennas and Propagation Magazine*, vol. 57, no. 2, pp. 145–152, 2015.

[33] W.-Q. Wang, "Overview of frequency diverse array in radar and navigation applications," *IET Radar, Sonar & Navigation*, vol. 10, no. 6, pp. 1001–1012, 2016.

[34] Y. Zhu, H. Wang, S. Zhang, Z. Zheng, and W. Wang, "Deceptive jamming on space-borne SAR using frequency diverse array," in *IGARSS 2018 - 2018 IEEE International Geoscience and Remote Sensing Symposium*, pp. 605–608, Valencia, Spain, 2018.

[35] B. Huang, W.-Q. Wang, S. Zhang, H. Wang, R. Gui, and L. Zheng, "A novel approach for spaceborne SAR scattered-wave deception jamming using frequency diverse array," *IEEE Geoscience and Remote Sensing Letters*, vol. 17, no. 9, pp. 1568–1572, 2020.

[36] W. Mao, H. Wang, S. Zhang, and X. Liu, "A novel deceptive jamming method via frequency diverse array," in *IGARSS 2019 - 2019 IEEE International Geoscience and Remote Sensing Symposium*, pp. 2369–2372, Yokohama, Japan, 2019.

[37] H. Wang, S. Zhang, W.-Q. Wang, B. Huang, Z. Zheng, and L. Zheng, "Multi-scene deception jamming on SAR imaging with FDA antenna," *IEEE Access*, vol. 8, pp. 7058–7069, 2019.

[38] Y. Liao, T. Hu, X. Chen et al., "Antenna Beampattern with range null control using weighted frequency diverse array," *IEEE Access*, vol. 8, pp. 50107–50117, 2020.